# Nonlinear optics of conjugated polymers: A coupled exciton-phonon-gas approach

F. X. Bronold* and A. R. Bishop
*Theoretical Division and Center for Nonlinear Studies, Los Alamos National Laboratory, Los Alamos, New Mexico 87545*
(Received 23 October 1995)

Conjugated polymers are modeled as a system of one-dimensional $\pi$ electrons interacting via a short-range Coulomb interaction and coupled to an underlying harmonic lattice, i.e., as an extended Peierls-Hubbard model. A perturbative bosonization procedure is employed to map the original Hamiltonian onto an effective one describing a coupled, one-dimensional exciton-phonon gas (EPG), which should be especially useful in discussing nonlinear optics. This approach treats excitons as ideal Bose (quasi)particles subject to effective interactions, which in turn are the microscopic origin of the nonlinear optics response of the material. In particular, we derive effective interaction vertices for (i) exciton-exciton scattering, (ii) exciton-phonon coupling, and (iii) (nonlinear) exciton-light coupling within a semiclassical approximation. As an application of the EPG model to nonlinear optics of conjugated polymers, we study, in the collisionless regime, the steady-state response of a coherently pumped EPG with respect to a spectrally broad test laser. The EPG approach discusses this particular four-wave-mixing experiment in terms of an externally driven, interacting two-component Bose gas. It explains optical Stark effects and inverse Raman scattering as due to composite excitations whose electronic and phononic degrees of freedom depend upon pump frequency and pump intensity. [S0163-1829(96)05320-9]

## I. INTRODUCTION

Conjugated polymers, such as polyacetylene (PA), polydiacetylenes (PDA), and poly(phenylene)vinylene (PPV), are quasi-one-dimensional (Q1D) organic semiconductors with good mechanical, e.g., flexibility, and excellent optoelectronic, e.g., large optical nonlinearities, properties. In contrast to inorganic semiconductors, e.g., GaAs, the properties of a particular polymer can be varied over a wide range by chemical means, e.g., by attaching different side groups or by blending two different polymers. It is especially the latter property of engineering the material properties by relatively straightforward and cheap chemical means that makes conjugated polymers very attractive for technological applications in general and optoelectronic devices in particular. Most previous application-oriented research centered around PDA-based optical wave guides[1] and all-optical switches.[2] Both applications rely on an intrinsic nonlinear optical process, namely, the change of the index of refraction with light intensity. In recent years, interest has moved to include PPV-based light-emitting diodes[3] employing electroluminescence of PPV and some of its derivatives. Since both PDA (Ref. 4) and PPV (Ref. 5) are characterized by a strong low-lying electronic excitation, a detailed understanding of the low-energy *energetics* and *dynamics* is a prerequisite for any well-controlled device design.

Consequently, there has been much effort, experimentally and theoretically, to understand the low-energy photophysics of conjugated polymers. In particular, time-resolved photo-induced absorption,[6] time-resolved four-wave mixing (FWM), and pump-and-probe techniques[7] constitute powerful and flexible approaches to probing the dynamics of photo-excitations down to very short-time scales. Especially the coherent pump-and-probe experiments, employing a non-resonant pump laser and thus creating virtual excitations, has attracted much interest.[4,8,9] It is well known from experiments with low-dimensional *inorganic* semiconductors, e.g., $GaAs/Al_xGa_{1-x}As$ multiple-quantum-well structures,[10] that for a detailed understanding and accurate interpretation of both steady-state and transient nonlinear optics response a sound many-body theoretical description is essential. It is therefore expected that a detailed understanding of nonlinear spectroscopy, as well as of the dynamics of photoexcitations in conjugated polymers, also requires a many-body theoretical description. This is even more true in view of the strong Coulomb interaction and electron-phonon coupling in this type of material.

This paper proposes such a many-body theoretical treatment of nonlinear optics effects considering conjugated polymers as Q1D semiconductors, i.e., we study conjugated polymers in the long-chain limit. Although most theoretical studies in the field of nonlinear optics of conjugated polymers use (nonlinear) susceptibilities to characterize the nonlinear optical response of the material — the $\chi_3$ formalism[11] — we adopt here a different approach that is more common in (inorganic) semiconductor physics. Namely, we discuss nonlinear optics in terms of renormalized quasiparticles and their coupling to external fields. In this sense it should be considered complementary to the $\chi_3$ formalism, although we suggest that our approach has some advantages in terms of transparency and flexibility.

Without going into mathematical details, the main points of our approach are as follows. *First*, before studying the coupling of the material to external, time-dependent (light) fields, we transform the Hamiltonian modeling a generic conjugated polymer into a representation that is more suitable to discuss nonlinear optics in terms of quasiparticles. We choose collective electron-hole pairs [viz., excitons in the Tamm-Dancoff approximation (TDA), i.e., Wannier excitons] and optical phonons as ''bare'' quasiparticles and explicitly derive effective interaction vertices between these

 

''undressed'' quasiparticles. A very transparent method of deriving effective interactions between excitons, i.e., between composite fermion pairs, and between excitons and phonons is a bosonization technique for bilinear fermion operators recently developed in nuclear structure theory by Sakamoto and Kishimoto.[12] Technically, we treat excitons as Bose particles with effective interaction vertices describing (i) exciton-exciton scattering, (ii) exciton-phonon scattering, and (iii) coupling to external fields.[13] In all three, vertex exchange corrections due to the Pauli principle are included. In a *second* step, we then consider the full problem of an externally driven (by light fields) conjugated polymer described by interacting excitons and phonons, i.e., by an exciton-phonon gas (EPG). For simplicity we consider pump-and-probe spectroscopy in the quasistationary approximation. We assume a pump pulse shorter than the relevant relaxation times, i.e., collisionsless regime, and calculate the steady-state response of the (nonresonantly) pumped EPG. As pointed out by Schmitt-Rink, Chemla, and Haug,[14] under these conditions there is a close analogy between optically pumped semiconducting structures and weakly interacting Bose gases. We closely follow Schmitt-Rink, Chemla, and Haug and discuss the optical Stark effect (OSE) and inverse Raman scattering (IRS) in terms of composite quasiparticles comprising excitonic and phononic degrees of freedom. Although our theory of the OSE and IRS is very rudimentary, we emphasize that more refined treatments are possible. In fact, most of the techniques developed in the field of collective excitations of superfluids[15] can, if appropriately modified, be applied to nonlinear optics as well.

The paper is organized as follows. Section II is devoted to deriving the coupled exciton-phonon-gas representation for conjugated polymers. In Sec. II A we introduce a generic model for conjugated polymers that models this class of materials as a one-dimensional system of interacting $\pi$ electrons coupled to a harmonic lattice. In Sec. II B we define bilinear fermion operators — exciton and scattering operators — and present their commutation rules. In Sec. II C we present an approximate boson expansion for these operators and finally express the original model in terms of two boson fields, one for excitons and the other for (optical) phonons. Particular emphasis is directed towards the discussion of effective interactions defining the EPG Hamiltonian. Section III gives a detailed theoretical description of (nonresonant) pump-and-probe spectroscopy in the collisionless regime. Using the EPG respresentation, we derive in Sec. III A equations that determine the coherent ground state of a pumped conjugated polymer. Section III B is then devoted to constructing equations to determine the excitation spectrum of the pumped EPG, which is subsequently used in Sec. III C to calculating the steady-state response to a weak test laser. In Sec. III D we present numerical results for the OSE and IRS. Section IV summarizes the paper and indicates some improvements to our approach that should enable us (i) to study transient response functions and (ii) to realistically treat biexciton formation and signatures in nonlinear optics experiments, e.g., two-photon absorption. For the sake of completeness and to specifiy our notation, we present in Appendixes A and B, closely following Hayashi and Nasu,[16] mathematical details for the mean-field approximation and particle-hole representation, respectively. Finally, Appendix C shows explicit expressions for the interaction vertices defining the coupled EPG.

TABLE I. Representative parametrization of the model Hamiltonian for PDA.

| $t_0$ (eV) | $\alpha$ (eV/Å) | $U$ (eV) | $V$ (eV) | $M$ (a.u.) | $K$ (eV/Å$^2$) |
|---|---|---|---|---|---|
| 2.5 | 3.6 | 5.0 | 2.5 | 13.0 | 21.0 |

## II. EXCITON-PHONON-GAS REPRESENTATION

### A. Model Hamiltonian

Although conjugated polymers are extremely complicated materials with many (coupled) degrees of freedom and, depending on the particular synthesis route, a considerable amount of structural imperfections and electronic disorder,[17] the optical properties of this class of materials are, to a large extent, determined by delocalized, multicenter bonds characteristic of unsaturated organic compounds: the $\pi$ electrons. Following common recent practice,[18] we will, therefore, consider a simple model Hamiltonian describing an extended $\pi$-electron system confined to one dimension, the polymer backbone, and neglect all the other degrees of freedom. Specifically, we will use a Su-Schrieffer-Heeger model[19] augmented by Hubbard $U$ and $V$ terms [i.e., a Peierls- (extended) Hubbard model] as a model for a *generic* conjugated polymer (the lattice constant is set to unity):

$$H=-\sum_{l,\sigma}\left[t_0-\alpha(u_{l+1}-u_l)\right]\left[c_{l\sigma}^{\dagger}c_{l+1\sigma}+\text{H.c.}\right]+U\sum_{l}n_{l\uparrow}n_{l\downarrow}+V\sum_{l,\sigma,\tau}n_{l\sigma}n_{l+1\tau}+\sum_{l}\left[\frac{M}{2}\dot{u}_l^2+\frac{K}{2}(u_{l+1}-u_l)^2\right]. \tag{1}$$

Here $c_{l\sigma}^{\dagger}$ creates an electron in a Wannier orbital at site $l$ with spin polarization $\sigma$ and $n_{l\sigma}=c_{l\sigma}^{\dagger}c_{l\sigma}$, the total charge on site $l$ with spin $\sigma$. The parameters $t_0$, $\alpha$, $U$, and $V$ are the $\pi$-electron hopping integral, the electron-phonon coupling, and the Hubbard parameters characterizing the short-range electron-electron interaction, respectively. $K$ and $M$ represent the lattice compressibility (due to $\sigma$ bonds) and the mass at each lattice site. Strictly speaking, the Hamiltonian Eq. (1) applies only to linear chain polymers with originally one atom (site) per unit cell. Recent work, however, has shown that the primary excitations in systems like PPV, and implicitly also like PDA, can be described within *effective* linear chain models of the form (1).[20] Representative model parameters for PDA are given in Table I. We study model (1) at half-filling with periodic boundary conditions and $N$ sites.

To complete our model description, we add a term that accounts for the coupling between $\pi$ electrons and light in a semiclassical approximation. Furthermore, we assume homogeneous irradiation of the polymer sample and write in the dipole approximation

$$\delta H_{\pi\ \text{light}}=-\sum_{l,\sigma}\mu_l c_{l\sigma}^{\dagger}c_{l\sigma}\mathscr{E}(t). \tag{2}$$

Here $\mu_l$ is the (electric) dipole moment and $\mathscr{E}(t)$ denotes the electric component of the light field along the polymer backbone. For simplicity, we neglect phonon-assisted coupling processes and take for the dipole moment

$$\mu_l = \frac{eN}{4\pi} \sin\frac{2\pi}{N}(l-1). \tag{3}$$

This particular form of the dipole moment has been used in the literature before[18] and ensures that periodic boundary conditions are satisfied and that in the large-$N$ limit the dipole moment aquires the canonical form $\mu_l = e(l-1)$. (Note that the origin of our coordinate system is $l=1$.)

For the investigation of optical processes it is convenient to rewrite model (1) in terms of particle and hole operators defined with respect to a suitable ground state. In order to be applicable to conjugated polymers, e.g., PA, PDA, and PPV, the model parameters ($t_0$, $U$, $V$, $\alpha$, $M$, and $K$) ought to be such that the ground state of model (1) is a bond-order wave (BOW), i.e., the ground state is a dimerized Peierls semiconductor with, at half filling, a full valence and an empty conduction band. In Appendix A we briefly review, primarily to specify our notation, the mean-field theory of model Eq. (1) in the BOW phase following Hayashi and Nasu.[16] In contrast to conventional inorganic semiconductors, the single-particle gap separating the full valence from the empty conduction band is due primarily to electron-phonon coupling (Peierls instability) further stabilized by the next-neighbor Coulomb interaction ($V$ term). As a consequence of the Peierls instability, the unit cell is doubled. Thus, instead of one (acoustic) phonon branch we have two phonon branches, one acoustic and one optic.

In the present context, the main result of the mean-field approximation is to transform model (1), which orginally described a one-dimensional metal, into a one-dimensional semiconductor with residual Coulomb and electron-phonon interactions. With respect to the semiconducting Peierls-dimerized ground state in the mean-field approximation, denoted by $|\mathscr{M}\rangle$, we then define particle (hole) operators (see also Appendix A) $p(h)_{k\sigma}|\mathscr{M}\rangle = 0$ and optic-phonon operators (we do not consider acoustic phonons) $b_q|\mathscr{M}\rangle = 0$. It is then straightforward to express model (1) in terms of these new operators, although the algebra involved is rather lengthy.[16] To fix our notation it suffices to relegate the main mathematical steps to Appendix B and to restrict ourself here to a discussion of the final result. In particular we point out which terms have been neglected and emphasize the physical meaning of the terms retained.

Let us first comment on the electronic part. We neglect all umklapp processes ($U$ processes) with respect to the unit cell of the dimerized lattice. Furthermore, we ignore the scattering of a particle (hole) on a polarization wave (particle-hole pair) as well as spontaneous creation of particle-hole pairs. The former can be incorporated into a proper dielectric constant,[21,22] whereas the latter is suppressed due to the single particle gap.[23] Thus, as far as the electronic part is concerned, we are left with the free [mean-field approximation (MFA)] dispersion for the particles and holes, particle-hole scattering giving rise to exciton formation and scattering within valence and conduction bands, which becomes increasingly important if a finite concentration of particle-hole pairs is created, e.g., by a pump laser.

Let us now turn to the phonon part. First of all, we do not consider acoustic phonons and keep only the optic branch. This is not to say that acoustic phonons do not affect optical experiments at all. In fact, they are very important for relaxation and equilibration processes[24] of hot carriers. Since we study pump-and-probe spectroscopy in the collisionless regime, i.e., we study processes faster than intrinsic relaxation times, we can in a first approximation neglect the effect of acoustic phonons and consider only the coupling of electronic excitations to optical phonons. In particular the optical phonon in the center of the Brillouin zone (BZ) ($q=0$) plays a key role for coherent inverse Raman scattering. Furthermore, we do not account for scattering processes where a (optical) phonon creates (annihilates) a particle-hole pair, i.e., interband scattering events. Clearly, these processes play a crucial role for the renormalization of (optic) phonons due to the polarizability of electrons. It is well known[25,26] that this leads to a significant softening of the $q=0$ optical phonon and can therefore be accounted for by a proper choice of the (optic-) phonon dispersion. Since we do not attempt to present a fully self-consistent theory of the rather complicated model (1), we use the bare (optic) phonon. For a more precise calculation one should, however, incorporate the renormalized phonon frequencies. Finally, the coupling to the light field is due only to creation (annihilation) of particle-hole pairs and not due to scattering events within the conduction (valence) band. For optics this approximation is reasonable.

With these caveats and approximations, the Hamiltonian that serves as the starting point for our investigation of nonlinear optics of conjugated polymers reads, in the particle-hole representation, up to a constant comprising the total MFA and the zero-point phonon energy,

$$\begin{aligned} H = & \sum_{k,\sigma} E_k [p^\dagger_{k\sigma} p_{k\sigma} + h^\dagger_{k\sigma} h_{k\sigma}] + \sum_q \omega(q) b^\dagger_q b_q \\ & - \frac{1}{N} \sum_{k_i,\sigma,\tau} V^{eh,d}_{1234}\, p^\dagger_{k_2\tau} h^\dagger_{-k_4\bar{\sigma}} h_{-k_1\bar{\sigma}} p_{k_3\tau} \\ & + \frac{1}{N} \sum_{k_i,\sigma,\tau} V^{eh,x}_{1234}\, p^\dagger_{k_2\tau} h^\dagger_{-k_3\bar{\tau}} h_{-k_1\bar{\sigma}} p_{k_4\sigma} \\ & + \frac{1}{2N} \sum_{k_i,\sigma,\tau} V^{pp}_{1234}\, p^\dagger_{k_1\sigma} p^\dagger_{k_2\tau} p_{k_3\tau} p_{k_4\sigma} \\ & + \frac{1}{2N} \sum_{k_i,\sigma,\tau} V^{hh}_{1234} h^\dagger_{-k_3\bar{\tau}} h^\dagger_{-k_4\bar{\sigma}} h_{-k_1\bar{\sigma}} h_{-k_2\bar{\tau}} \\ & + \sum_{k_1,k_2,q} \sum_\sigma W(k_1,k_2,q)[p^\dagger_{k_1\sigma} p_{k_2\sigma} + h^\dagger_{-k_2\bar{\sigma}} h_{-k_1\bar{\sigma}}] \\ & \times (b_q + b^\dagger_{-q}) + \sum_{k,\sigma} [\overline{\mu^{(2)}} p^\dagger_{k\sigma} h^\dagger_{-k\bar{\sigma}} + \text{H.c.}] \mathscr{E}(t), \end{aligned} \tag{4}$$

with $i = k_i$, e.g., $V^{w()}_{1234} \hat{=} V(k_1,k_2,k_3,k_4)^{()}$. Momentum sums are over the *reduced* BZ corresponding to the unit cell of the dimerized lattice, i.e., $-\pi/2 \leqslant k < \pi/2$. In terms describing the Coulomb interaction they are constrained to

$k_1+k_2=k_3+k_4$, while in the term denoting electron-phonon coupling the momentum sum is restricted to $k_1-k_2=q$. Notice that (4) describes *excitations* of the polymer whose energies are measured with respect to the total BOW ground-state energy (set to zero). The first two terms on the right-hand side (rhs) describe the free motion of particles, holes, and (optic) phonons. The next four terms depict (direct) particle-hole scattering, (exchange) particle-hole scattering, particle-particle, and hole-hole scattering, respectively. The last two terms represent the particle (-hole)-phonon interaction and the coupling to external (light) fields. $p^\dagger_{k\sigma}$ creates an electron with momentum $k$, spin polarization $\sigma$, and energy $E_k$ in the (MFA) conduction band, whereas $h^\dagger_{k\sigma}$ destroys an electron with momentum $-k$, spin polarization $-\sigma$, and energy $E_{-k}=E_k$ in the (MFA) valence band. $b^\dagger_q$ is the creation operator for an optical phonon with momentum $q$ and energy $\omega(q)$. The electronic mean-field dispersion $E_k$ and the phonon dispersion $\omega(q)$ are given in Appendix A, Eqs. (A26) and (A18). The matrix elements $V^{eh,d}_{1234}$, $V^{eh,x}_{1234}$, $V^{pp}_{1234}$, $V^{hh}_{1234}$, $W(k_1,k_2,q)$, and $\overline{\mu^{(2)}}$ are defined in Appendix B, Eqs. (B7), (B8), (B10), (B11), (B21), and (B26), respectively.

### B. Exciton and scattering operators

The main objective of this paper is to discuss optical processes of an organic semiconductor in the presence of a finite concentration of excitons (and, due to electron-phonon coupling, a finite number of stimulated phonons) generated by a strong pump laser. Under these conditions the usual strategy to calculate excitonic absorption using the TDA for the two-time two-body Green function in the particle-hole channel[27] breaks down even without phonons. Considering the electronic problem alone, the reason is that TDA treats collective particle-hole pairs, i.e., excitons, as bosons without internal structure. Clearly, the internal structure matters only for concentrations when excitons begin to overlap. There are many different ways to treat excitons beyond the *quasiboson approximation* inherent in TDA with no significant advantage to any of them. Here we have chosen an algebraic technique to study optical processes at finite exciton (and phonon) concentration: First, we employ an algebraic boson expansion that treats excitons as bosons with effective interactions taking their internal structure into account and, second, a unitary transformation approach to obtain the optical response of an optically pumped organic semiconductor in the mean-field approximation. To incorporate many-body correlations beyond the mean-field approximation it is, however, necessary to use more sophisticated methods, e.g., (bosonized) exciton Green functions.[30]

We exclusively restrict our theory to the singlet sector of the Hamiltonian (4) and base our treatment on bilinear fermionic operators that create (annihilate) collective, singlet particle-hole pairs, i.e., singlet excitons, defined by

$$S^\dagger_{Q\mu}=\sum_{k,q}\ \delta_{Q,k+q}\Phi^\mu_Q\left(\frac{k-q}{2}\right)S^\dagger_{kq}, \tag{5}$$

with

$$S^\dagger_{kq}=\frac{1}{\sqrt{2}}[p^\dagger_{k\uparrow}h^\dagger_{q\downarrow}+p^\dagger_{k\downarrow}h^\dagger_{q\uparrow}]. \tag{6}$$

Here $S^\dagger_{Q\mu}$ creates a singlet exciton with total (crystal) momentum $Q$ and internal quantum number $\mu$. Obviously, $|\mathscr{M}\rangle$ is the vacuum for exciton operators. The coefficient $\Phi^\mu_Q(q)$ is the exciton wave function as obtained, for instance, from the solution of the Bethe-Salpeter equation in the TDA. The index $\mu$ encompasses the whole spectrum of the two-body problem: bound states and scattering states. In this sense, we use the word ''exciton'' in an unconventional way, calling both bound and unbound particle-hole pairs excitons. $q$ depicts the momentum associated with the relative motion of the particle-hole pair. In Appendix C we will show that a natural choice for $\Phi^\mu_Q(q)$ is indeed the solution of the Bethe-Salpeter equation in the TDA, which in the present context leads to the Wannier equation for excitons based on model (4); it diagonalizes the leading term of the resulting EPG Hamiltonian in the dilute limit.

Additionally, we introduce for technical reasons particle and hole *scattering operators*

$$C^\dagger_{kq}=\sum_\sigma\ p^\dagger_{k\sigma}p_{q\sigma}, \tag{7}$$

$$D^\dagger_{kq}=\sum_\sigma\ h^\dagger_{k\sigma}h_{q\sigma}. \tag{8}$$

The operators (5), (7), and (8) statisfy commutation relations

$$[S_{K\nu},S^\dagger_{Q\mu}]=\delta_{KQ}\delta_{\nu\mu}-\frac{1}{2}\sum_l\ P^+_{K\nu;Q\mu}(l,l)C^\dagger_{Q-l,K-l}$$
$$-\frac{1}{2}\sum_l\ P^-_{K\nu;Q\mu}(l,l)D^\dagger_{Q-l,K-l}, \tag{9}$$

$$[C^\dagger_{kq},S^\dagger_{K\nu}]=\sum_{Q,\mu}\ P^-_{K\nu;Q\mu}(q,k)\,\delta_{Q,K+k-q}S^\dagger_{Q\mu}, \tag{10}$$

$$[D^\dagger_{kq},S^\dagger_{K\nu}]=\sum_{Q,\mu}\ P^+_{K\nu;Q\mu}(q,k)\,\delta_{Q,K+k-q}S^\dagger_{Q\mu}, \tag{11}$$

$$[S_{K\nu},S_{Q\mu}]=0, \tag{12}$$

$$[C^\dagger_{kq},D^\dagger_{\tilde{k}\tilde{q}}]=0, \tag{13}$$

with *structure coefficients*, anticipating exciton wave functions to be real,

$$P^+_{K\nu;Q\mu}(k,q)=\Phi^\nu_K\left(\frac{K}{2}-k\right)\Phi^\mu_Q\left(\frac{Q}{2}-q\right), \tag{14}$$

$$P^-_{K\nu;Q\mu}(k,q)=\Phi^\nu_K\left(-\frac{K}{2}+k\right)\Phi^\mu_Q\left(-\frac{Q}{2}+q\right). \tag{15}$$

If it were not for the last two terms on the rhs of Eq. (9) exciton operators would satisfy Bose statistics. Taking the expectation value of Eq. (9), we see, however, that corrections to Bose statistics are linked to the density of particle-hole pairs. In the case of a vanishing pair density we can

therefore neglect the operators on the rhs of Eq. (9) and treat excitons as ideal Bose particles without internal structure leading to the TDA for particle-hole pairs and eventually to the Wannier equation. At finite density the full commutator relations have to be taken into account. In order to find a boson representation for the electronic subsystem of model (4) it is advantageous to express (4) in terms of the operators $S^\dagger_{Q\mu}$, $C^\dagger_{kq}$, and $D^\dagger_{kq}$. Employing definitions (5), (7), and (8), we immediately find

$$\begin{aligned} H=&\sum_k E_k[C^\dagger_{kk}+D^\dagger_{kk}]+\sum_q \omega(q)b^\dagger_q b_q \\ &+\sum_{K,Q}\sum_{\nu,\mu} V^{\mathrm{TDA}}_{\nu\mu}(K)\delta_{KQ}S^\dagger_{K\nu}S_{Q\mu} \\ &+\frac{1}{2N}\sum_{k_i} V^{pp}_{1234}C^\dagger_{k_1k_4}C^\dagger_{k_2k_3}-\frac{1}{2N}\sum_{k_i} V^{pp}_{1234}\delta_{k_2k_4}C^\dagger_{k_1k_3} \\ &+\frac{1}{2N}\sum_{k_i} V^{hh}_{1234}D^\dagger_{-k_3-k_2}D^\dagger_{-k_4-k_1} \\ &-\frac{1}{2N}\sum_{k_i} V^{hh}_{1234}\delta_{k_2k_4}D^\dagger_{-k_3-k_1} \\ &+\sum_{k_1,k_2,q} W(k_1,k_2,q)[C^\dagger_{k_1k_2}+D^\dagger_{-k_2,-k_1}](b_q+b^\dagger_{-q}) \\ &-\sum_\nu (\mu_\nu S_{0\nu}+\mathrm{H.c.})\mathscr{E}(t), \end{aligned} \tag{16}$$

with

$$\mu_\nu=\sqrt{2}\sum_q \Phi^\nu_0(q)\overline{\mu^{(2)}}, \tag{17}$$

$$V^{\mathrm{TDA}}_{\nu\mu}(K)=\sum_{q,r}\Phi^\nu_K(q)G_K(qr)\Phi^\mu_K(r), \tag{18}$$

and the symmetric $(N/2\times N/2)$ matrix

$$\begin{aligned} G_K(qr)=&G_K(rq) \\ =&-\frac{1}{N}\left[V^{eh,d}\left(-\frac{K}{2}+r,\frac{K}{2}+q,\frac{K}{2}+r,-\frac{K}{2}+q\right)\right. \\ &\left.-2V^{eh,x}\left(-\frac{K}{2}+r,\frac{K}{2}+q,-\frac{K}{2}+q,\frac{K}{2}+r\right)\right]. \end{aligned} \tag{19}$$

The remaining vertices and the dispersion for both phonons and (mean-field) quasiparticles (holes) can be found, as indicated in Sec. II A, in Appendixes A and B. Before we turn to the approximate bosonization of (16) we wish to comment on our restriction to singlet excitons. The (half-filled) ground state is a spin singlet. Due to selection rules the absorption of light leads to the creation of singlet excitons. As far as linear absorption is concerned, triplet excitons are therefore forbidden and it suffices to exclusively restrict the theory to the singlet sector. At finite exciton densities this is, however, no longer clear. Singlet and triplet exciton operators denote not truly independent excitations, which can be seen, for instance, from the commutator

$$\begin{aligned} [S_{K\nu},T^\dagger_{Q\mu 1}]=&-\frac{1}{\sqrt{2}}\sum_l \Phi^\nu_K\left(\frac{K}{2}-l\right)\Psi^\mu_Q\left(\frac{Q}{2}-l\right)p^\dagger_{Q-l\uparrow}p_{K-l\downarrow} \\ &-\frac{1}{\sqrt{2}}\sum_l \Phi^\nu_K\left(-\frac{K}{2}+l\right) \\ &\times\Psi^\mu_Q\left(-\frac{Q}{2}+l\right)h^\dagger_{Q-l\uparrow}h_{K-l\downarrow}, \end{aligned} \tag{20}$$

with the $m=1$ triplet exciton defined by

$$T^\dagger_{Q\mu 1}=\sum_{k,q}\delta_{Q,k+q}\Psi^\mu_Q\left(\frac{k-q}{2}\right)T^\dagger_{kq1} \tag{21}$$

and

$$T^\dagger_{kq1}=p^\dagger_{k\uparrow}h^\dagger_{q\uparrow}. \tag{22}$$

Here $\Psi^\mu_Q(q)$ is the wave function for a triplet exciton corresponding to the solution of the Bethe-Salpeter equation for the two-time two-body Green function in the triplet particle-hole channel.[30] Clearly, the operators on the rhs of Eq. (20) flip the spin of a particle and a hole, respectively, and their expectation values in a finite density exciton gas are zero as long as we allow only spin-conserving scattering processes. Additonally, particle-hole symmetry also plays an important role in determining whether singlet and triplet sectors are indeed decoupled or not. Since in the high-density regime excitons are ionized, it is conceivable that triplet and singlet sectors are not strictly decoupled. This is even more problematic if the finite lifetime of excitons is taken into account with different decay channels for singlet and triplet excitations. In the following we assume, however, (i) that excitons created by the pump laser have, as far as experimental timescales are concerned, ''infinite'' lifetimes and (ii) that the ground state of the pumped organic semiconductor is not too far from the BOW ground state, i.e., from $|\mathscr{M}\rangle$. Under these restrictions it is appropriate to neglect the triplet sector.

### C. Approximate boson representation

Up to this point there was nothing new in our treatment of the extended Peierls-Hubbard model and all we have done is to rewrite the original Hamiltonian in terms of exciton, scattering, and phonon operators defined with respect to the semiconducting Peierls-dimerized ground state of model (1). Recall, however, that on the way from (1) to (16) we neglected certain terms that we consider as unimportant for the investigation of optical properties of conjugated polymers, e.g., acoustic phonons or $U$ processes. Since we otherwise carefully kept residual interactions, no serious approximations have yet been made.

Physically speaking, Eq. (16) still describes a system of coupled electrons and phonons driven by an external (light) field and to study the optical properties of this rather com-

plicated model we could derive equations of motion for $S^{\dagger}_{Q\mu}$, $C^{\dagger}_{kq}$, $D^{\dagger}_{kq}$, and $b^{\dagger}_{q}$ similar to density-matrix approaches.[28] In these approaches one encounters the problem of decoupling expectation values such as $\langle S^{\dagger}_{K\mu} D^{\dagger}_{kq}\rangle$, which is far from trivial. In most of these approaches an *implicit* bosonization has been applied so that it is natural to express (16) in terms of boson fields from the start and then use either equations of motion or other many-body techniques to study the optical reponse in the EPG representation.

We apply a perturbative bosonization technique for fermion-pair operators developed in nuclear structure theory, which enables us to express fermionic pair operators as infinite polynomials of boson operators (viz., infinite series of normally ordered products of boson operators).[12] Although the physics involved is quite simple, due primarily to the microscopic nature of the technique, the notations and formal manipulations are nevertheless very involved. For technical details and a discussion of mathematical subtleties we therefore refer the reader to the original papers by Sakamoto and Kishimoto[12,29] and to Ref. 30. For the purpose of this paper it suffices to recall the main points. First, it is important to note that instead of expanding bare fermion pairs, e.g., $S^{\dagger}_{kq}$, collective fermion pairs, i.e., $S^{\dagger}_{K\nu}$, are expressed in terms of a Taylor series of normally ordered products of boson operators. Thus minimal dynamical studies have been done in the fermion space and hopefully the most important correlations have been summed up exactly. Specifically, it is convenient to determine collective pairs, i.e., excitons, within the TDA for the Bethe-Salpeter equation in the (singlet) particle-hole channel. In quantum chemical terms, this procedure is equivalent to a single−configuration-interaction calculation. Second, once the collective pairs have been defined, the mapping procedure (from fermion to boson space) is a purely *kinematic* problem,[31] in the sense that only the algebra obeyed by $S^{\dagger}_{K\nu}$, $C^{\dagger}_{kq}$, and $D^{\dagger}_{kq}$, Eqs. (9)–(13), matters. Despite mathematical subtleties it can be shown that infinite, normally ordered boson polynomials constructed in a systematic procedure employing an Usui operator[12] satisfy the algebra obeyed by the original fermion pair operators, i.e., matrix elements as well as equations of motion are conserved. Unfortunately, from a practical point of view the polynomials have to be truncated at some order. In particular, we present here only the lowest-order polynomials for $S^{\dagger}_{K\nu}$, $C^{\dagger}_{kq}$, and $D^{\dagger}_{kq}$ and leave a detailed discussion of convergence properties aside. The interested reader is invited to consult Refs. 12, 29, and 30 for more details.

In terms of boson operators, we can write for the exciton operator

$$(S^{\dagger}_{Q\mu})_B = A^{\dagger}_{Q\mu} - \frac{1}{4}\sum_{K_1,\nu_1,K_2,\nu_2,K_3,\nu_3} Y(Q\mu;K_1\nu_1K_2\nu_2K_3\nu_3) \times \delta_{Q,K_1+K_2-K_3} A^{\dagger}_{K_1\nu_1}A^{\dagger}_{K_2\nu_2}A_{K_3\nu_3} + O(Y^2), \quad (23)$$

where the *rearrangement coefficient*, which in fact is the expansion parameter, reads

$$Y(Q_1\mu_1;K_1\nu_1K_2\nu_2K_3\nu_3) = +\frac{1}{2}\sum_{l} P^{+}_{K_1\nu_1;Q_1\mu_1}(l,l)P^{-}_{K_2\nu_2;K_3\nu_3}(Q_1-l,K_1-l) + \frac{1}{2}\sum_{l} P^{-}_{K_1\nu_1;Q_1\mu_1}(l,l)P^{+}_{K_2\nu_2;K_3\nu_3}(Q_1-l,K_1-l). \quad (24)$$

It is easy to verify that $Y$ accounts for the deviation of the overlap of two-exciton states from the corresponding overlap of two-boson states. Thus $Y$ takes care of the internal structure of excitons.[30] The scattering operators can be expressed as bilinear boson forms

$$(C^{\dagger}_{kq})_B = \sum_{K,\nu}\sum_{Q,\mu} P^{-}_{K\nu;Q\mu}(k,q)\,\delta_{K,Q+k-q} A^{\dagger}_{K\nu}A_{Q\mu}, \quad (25)$$

$$(D^{\dagger}_{kq})_B = \sum_{K,\nu}\sum_{Q,\mu} P^{+}_{K\nu;Q\mu}(k,q)\,\delta_{K,Q+k-q} A^{\dagger}_{K\nu}A_{Q\mu}. \quad (26)$$

The structure coefficients $P^{\pm}$ entering Eqs. (24)–(26) are defined in Eqs. (14) and (15).

Using Eqs. (23), (25), and (26), we can then express model (16) in terms of two boson fields, namely, one field for optical phonons $b_q \rightarrow B_Q$ and another field for excitons $A_{K\mu}$. In Appendix C we will give details of this straightforward procedure. Finally, we obtain a Hamiltonian that describes a conjugated polymer (i.e., PA, PDA, or PPV) coupled to external light fields as a *coupled exciton-phonon gas* driven by external time-dependent electric fields. Specifically, the EPG Hamiltonian — the final result of Sec. II — reads

$$\mathscr{H} = \sum_{K,\nu}\Omega_{\nu}(K)A^{\dagger}_{K\nu}A_{K\nu} + \sum_{Q}\omega(Q)B^{\dagger}_{Q}B_{Q} + \sum_{K_i,\nu_i}\delta_{K_1+K_2,K_3+K_4}\mathscr{W}_{1234}A^{\dagger}_{1}A^{\dagger}_{2}A_{3}A_{4} + \sum_{K,Q}\sum_{\nu,\mu}\mathscr{M}_{\nu\mu}(K;Q)A^{\dagger}_{K+Q\nu}A_{K\mu}(B_Q+B^{\dagger}_{-Q}) - \sum_{\nu}(\mu_{\nu}A_{0\nu}+\text{H.c.})\mathscr{E}(t) + \sum_{K_i,\nu_i}\tilde{\mu}(K_1\nu_1K_2\nu_2K_3\nu_3) \times \delta_{K_3,K_1+K_2}[A^{\dagger}_{K_1\nu_1}A^{\dagger}_{K_2\nu_2}A_{K_3\nu_3}+\text{H.c.}]\mathscr{E}(t), \quad (27)$$

with $i=K_i\nu_i$. Here $\omega(Q)$ and $\Omega_{\nu}(K)$ depict, respectively, the optic-phonon branch defined in Appendix A, Eq. (A18), and the TDA disperison for singlet excitons given by the solution of Eq. (C2) in Appendix C. Explicit expressions for the interaction vertices are provided in Appendix C, Eqs. (C8), (C10), and (C13), while the dipole moment $\mu_{\nu}$ is defined in Eq. (17). Both fields, the exciton and the phonon, satisfy Bose statistics and are independent of each other. The first two terms on the rhs of Eq. (27) represent the free motion of TDA particle-hole pairs (excitons) and phonons. The

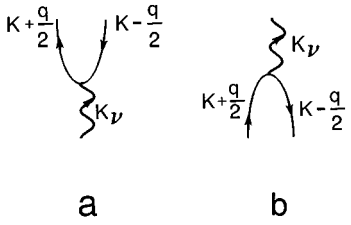


FIG. 1. Graphical representation of TDA wave functions $\Phi_K^\nu(q)$: (a) annihilation of a TDA pair and (b) creation of a TDA pair.

third and fourth terms describe, respectively, exciton-exciton and exciton-phonon scattering; both give rise to optical nonlinearities. The last two terms stand for linear and nonlinear coupling to classical light fields.

Since the analytic expressions for the various vertices defining our EPG model are rather complicated, which might obscure the simple physics they contain, we present in Figs. 3–5 these vertices graphically in terms of mode-mode-coupling diagrams.[32] We emphasize that these ''diagrams'' are not Feynmann diagrams in the canonical sense and we use them only to make the rather complicated analytic expressions of Appendix C transparent and to provide some insight into the physics contained in the EPG Hamiltonian (27). In Sec. III we apply ordinary perturbation theory to obtain the nonlinear response of the optically pumped EPG. It is then important to keep in mind that the interaction vertices, albeit depicted as black boxes, are in fact composite entities with a complicated internal structure.

Let us represent the exciton wave funtion $\Phi_K^\nu(q)$ as a wavy up-going line that merges into a particle (up-going) line and a hole (down-going) line. The exciton line is labeled by the total (crystal) momentum $K$ and the internal quantum number $\nu$, whereas the particle and hole carry $K+q/2$ and $K-q/2$, respectively. As shown in Fig. 1, we can interpret $\Phi_K^\nu(q)$, assuming an artifical time going upward, as an annihilation of an exciton and, correspondingly, $\Phi_K^\nu(q)^*$ as a creation of an exciton. In fact, we will choose exciton wave functions to be real, but to give ''rules'' for constructing mode-mode coupling diagrams it is helpful to work with complex wave functions. Additionally, we represent $V^{\mathrm{TDA}}$, Eq. (18), as shown in Fig. 2. Note that, although $V^{\mathrm{TDA}}$ is diagonal in $K$ space, it is still nondiagonal in terms of the internal quantum numbers $\mu$ and $\nu$.

With Figs. 1 and 2 as building blocks, the exciton-exciton vertex Eq. (C8) can be represented as shown in Fig. 3 and consists of three parts: (i) the Pauli correction to the TDA result (the first two and last two terms), (ii) the particle-particle scattering (the third term), and (iii) the hole-hole scattering (the fourth term). As expected, the interaction of excitons due to the Pauli principle is given by the rearrangement coefficient $Y$. The remaining two processes describe


FIG. 2. Graphical representation of $V_{\nu\mu}^{\mathrm{TDA}}(K)$.

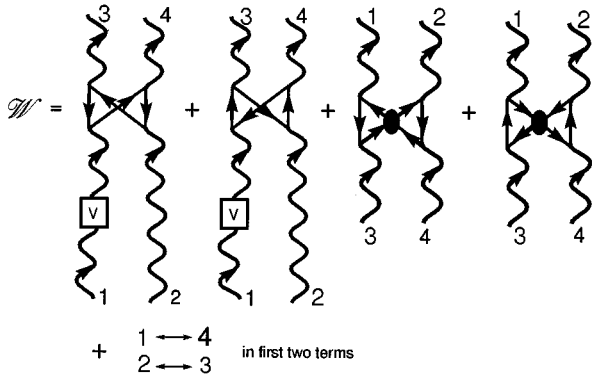


FIG. 3. Graphical representation of the exciton-exciton vertex. The first two and the last two terms represent exchange corrections to the TDA result. The third and fourth terms describe, respectively, particle-particle and hole-hole scattering.

the exciton-exciton interaction due to the Coulomb interaction. Specifically, the third term can be interpreted as an exciton-exciton scattering event where only the particles are subject to the Coulomb interaction: Two TDA modes decay with the holes traveling unperturbed (exchange), whereas the particles scatter on the Coulomb potential. Finally, particles and holes combine to form two (new) TDA modes. The situation is similar for hole-hole scattering (the fourth term), except that now particles travel without scattering. It is easy to check that momentum conservation given by the Kronecker delta function in Eq. (C8) is satisfied with our particular choice of diagrams for the exciton wave function. The black circle stands for the (short-range) particle-particle and hole-hole potentials $V^{pp}$ and $V^{hh}$, respectively.

The exciton-phonon vertex Eq. (C10) contains scattering of particles and scattering of holes and is represented in Fig. 4. Again, it is easy to check that momentum is conserved. The gray circle stands for the electron-phonon vertex and the zigzag line for an optical phonon. Figure 4(a) shows the decay of a TDA mode into its constituent particle and hole, subsequent scattering of the particle on a (optical) phonon, and, finally, the merging of the scattered particle with the unperturbed traveling hole to form a new TDA mode. In Fig. 4(b), the role of the particle and hole is interchanged.

Finally, we consider exciton-light interaction Eqs. (17) and (C13). Both the linear and the nonlinear terms act like source or sink terms for excitons since they do not conserve

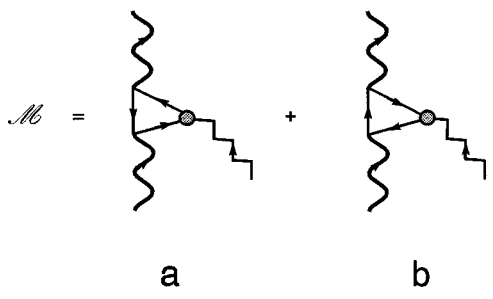


FIG. 4. Graphical representation of the exciton-phonon vertex: (a) particle-phonon scattering and (b) hole-phonon scattering.

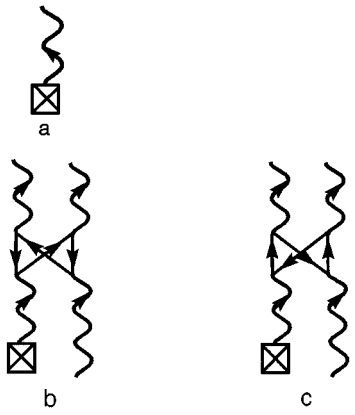


FIG. 5. Graphical representation of exciton-light vertices. (a) denotes linear exciton-light coupling. Nonlinear exciton-light coupling is depicted in (b) (particle exchange) and (c) (hole exchange).

the number of excitations. We will depict only the source terms; the box with a cross in it stands for the interaction with the (classical) light field. The linear term is trivially represented by Fig. 5(a) and needs no further comment; it is simply the creation of an exciton. The nonlinear terms are symbolized in Figs. 5(b) and 5(c). Clearly, it can be interpreted as the creation of an exciton due to the light field and subsequent decay of this exciton into a particle and a hole. Then exchange interactions with already existing excitons occur. Figure 5(b) depicts particle exchange and Fig. 5(c) hole exchange. Finally, recombination takes place and two excitons leave the vertex. Obviously, these processes are due purely to statistics and, moreover, take place only at finite density. This is the well-known phase-space filling effect,[33] which is included in our boson representation in the form of a *nonlinear* exciton-light interaction.

## III. HAMILTONIAN THEORY OF (NONRESONANT) PUMP-AND-PROBE SPECTROSCOPY

Within the simple conceptual frame of considering excitons as Bose particles with residual interaction among themselves, due to the Coulomb interaction and Pauli principle, and residual interaction with phonons, the following analogy of (nonresonant) pump-and-probe spectroscopy and weakly interacting Bose gases emerges.[14] The nonresonant (strong) pump laser creates a *virtual* ''condensate'' of pump-induced excitons and pump-stimulated optical phonons. Within the rotating-wave approximation, the pump frequency $\omega_p$ acts like a ''chemical potential'' that pins the condensate, thus opening the door to a quasi-equilibrium description of this involved many-body problem. Residual interactions ''deplete the condensate'' and renormalize the excitation spectrum of the pumped EPG seen by the second (weak) test laser. Specifically, excitations above the condensate are *composite quasiparticles* whose excitonic and phononic components, and thus the coupling to the test laser, are determined by pump frequency and intensity. In this section we present the lowest-order calculation for the optical Stark effect and inverse Raman scattering in close analogy to Bogoliubov's theory of a weakly interacting Bose gas. Specifically, we describe the ground state of the pumped EPG as a coherent superposition of excitons and phonons and the excitations in terms of a bilinear form of shifted exciton and phonon operators (viz., Hamiltonian theory), which can be diagonalized by a Bogoliubov transformation leading to composite quasiparticles, which in turn couple to the test laser and give rise to OSE and IRS.

### A. The coherent ground state

We consider a pump field (frequency $\omega_p$ below the optical gap) and a test field ($\mathscr{E}_t \ll \mathscr{E}_p$) of the form

$$\mathscr{E}(t) = \mathscr{E}_p e^{-i\omega_p t} + \mathscr{E}_t e^{-i\omega_t t} + \text{c.c.} \tag{28}$$

Since the frequency of the pump field $\omega_p$ is below the optical gap, only *virtual* particle-hole pairs (i.e., excitons) are created. In contrast to *real* particle-hole pairs whose lifetime is determined by *intrinsic* equilibration mechanisms, such as exciton-exciton and/or exciton-phonon scattering, the lifetime of virtual excitations is exclusively determined by the offset of the pump frequency from the lowest optical transition. Thus, according to Heisenberg's uncertainty principle, excitons created by the (nonresonant) pump laser have a lifetime roughly given by

$$\Delta\tau \sim \frac{h}{\Omega_1 - \omega_p}, \tag{29}$$

where $\Omega_1$ denotes the lowest exciton transition (optical gap). If, on the other hand, intrinsic scattering mechanisms giving rise to, e.g., (polarization) dephasing, occur on a time scale $T_x \gg \Delta\tau$, lifetimes of pump-induced excitons can be ignored. Hence the pump laser creates excitons *coherently*. In the following we will adopt a quasistationary approximation and neglect all dynamic aspects associated with pump-induced excitons and, due to exciton-phonon interaction, with pump-stimulated phonons. Our *collisionless* theory applies, therefore, to experiments with a smooth, ultrashort (compared to exciton lifetimes), and sufficiently nonresonant pump laser pulse. For more details about the validity of the quasistationary theory we refer to Ref. 34.

For the lowest-order theory of OSE and IRS we need to consider only excitons and phonons with total momentum $K=0$. Excitons and phonons with finite momentum appear only in higher order, e.g., in the $T$ matrix for multiple exciton scattering, which would be necessary for a proper description of biexcitons and their optical signatures. In the rotating frame of the pump laser, the EPG Hamiltonian (27), neglecting fast oscillating terms $\sim e^{-it2\omega_p}$ or $\sim^{-it(\omega_t+\omega_p)}$, reduces therefore to

$$\begin{aligned}\mathscr{H} = &\sum_{\nu} [\Omega_\nu - \omega_p] A_\nu^\dagger A_\nu + \omega_0 B^\dagger B \\ &+ \sum_{\nu,\mu,\lambda,\kappa} \mathscr{V}_{\nu\mu\lambda\kappa} A_\nu^\dagger A_\mu^\dagger A_\lambda A_\kappa + \sum_{\nu,\mu} \mathscr{M}_{\nu\mu} A_\nu^\dagger A_\mu (B + B^\dagger) \\ &- \sum_{\nu} (\mu_\nu A_\nu [\mathscr{E}_p + \mathscr{E}_t e^{-i\Delta t}] + \text{H.c.}) \\ &+ \sum_{\nu,i} (\tilde{\mu}_{\nu\mu\lambda} A_\nu^\dagger A_\mu^\dagger A_\lambda [\mathscr{E}_p + \mathscr{E}_t e^{-i\Delta t}] + \text{H.c.}),\end{aligned} \tag{30}$$

with $\Delta=\omega_t-\omega_p$ (offset between pump and test frequency), $\Omega_\nu=\Omega_\nu(0)$, $\omega_0=\omega(0)$, $A_\nu=A_{0\nu}$, and $B=B_0$. The interaction vertices are obtained from the general expressions given in Appendix C, Eqs. (C8), (C10), and (C13), by setting all momenta to zero. Since no confusion is possible, we will from now on suppress the momentum label for the exciton wave functions. After some algebra the (symmetrized) exciton-exciton vertex reads

$$\begin{aligned}\mathscr{V}_{\nu\mu\lambda\kappa}&=\frac{1}{4}[\mathscr{W}_{\nu\mu\kappa\lambda}+\mathscr{W}_{\mu\nu\kappa\lambda}+\mathscr{W}_{\nu\mu\lambda\kappa}+\mathscr{W}_{\mu\nu\lambda\kappa}]\\&=\frac{1}{8}\sum_q\,[8E_q-\Omega_\nu-\Omega_\mu-\Omega_\lambda-\Omega_\kappa]\\&\quad\times\Phi^\nu(q)\Phi^\mu(q)\Phi^\lambda(q)\Phi^\kappa(q)\\&\quad+\frac{u+2v}{2N}[\delta_{\nu\lambda}\delta_{\mu\kappa}+\delta_{\kappa\nu}\delta_{\lambda\mu}],\end{aligned}\tag{31}$$

with $\mathscr{W}_{\nu\mu\kappa\lambda}=\mathscr{W}_{0\nu0\mu0\kappa0\lambda}$. For the exciton-phonon vertex we find

$$\begin{aligned}\mathscr{M}_{\nu\mu}&\equiv\mathscr{M}_{\nu\mu}(0;0)\\&=-8\lambda\sqrt{\frac{1}{2\delta\omega_0 N}}\sum_q\,\sin(q)\frac{\Delta_q}{2E_q}\Phi^\nu(q)\Phi^\mu(q),\end{aligned}\tag{32}$$

with $E_q$ and $\Delta_q$ given in Appendix A, Eqs. (A26) and (A11), respectively, and $N$ the number of sites. The nonlinear coupling to the light fields is given by

$$\tilde{\mu}_{\nu\mu\lambda}\equiv\tilde{\mu}(0\nu0\mu0\lambda)=\frac{1}{4}\sum_{\kappa,q}\,\mu_\kappa\Phi^\nu(q)\Phi^\mu(q)\Phi^\lambda(q)\Phi^\kappa(q).\tag{33}$$

Employing definition (17), we find for the dipole matrix element

$$\mu_\nu=\sqrt{2}\frac{e}{2t_0}\sum_l\,\Phi^\nu(l),\tag{34}$$

which describes the linear exciton-light coupling. For simplicity we performed a gauge transformation $A_\nu^\dagger\to iA_\nu^\dagger$, which allows us to work with a real dipole matrix element [instead of with Eq. (B26)]. $\Phi_Q^\mu(q)$ and $\Omega_\nu$ denote the exciton wave function and exciton energy, respectively, as obtained in Appendix C by solving the Bethe-Salpeter equation in the TDA, i.e., Eq. (C2).

In the rotating frame, neglecting the envelope of the pump pulse, the pump field acts like a time independent source (sink) for excitons; only the coupling to the test laser is still time dependent. Therefore the ground state of the joint system of pump field, excitons, and phonons is no longer $|\mathscr{M}\rangle$ as specified in Eq. (A27), Appendix A. Instead, the ground state of the pumped system contains a finite number of excitons (particle-hole pairs) as well as phonons and is conveniently expressed in terms of a coherent state corresponding to a (unitary) Glauber transformation of Eq. (30). Using standard notation,[35] we write, for the ground state of the pumped EPG in the rotating frame,

$$|z;\gamma\rangle=U_G|\mathscr{M}\rangle\equiv\exp\left(\sum_\nu\,[A_\nu^\dagger z_\nu-hc]\right)e^{[B^\dagger\gamma-hc]}|\mathscr{M}\rangle,\tag{35}$$

where $|\mathscr{M}\rangle$ denotes the vacuum of the exciton operators $A_\nu$ (full valence and empty conduction band) and the vacuum of the phonon operator $B$ (dimerized lattice). As usual, the (unitary) Glauber transformation $U_G$ introduces new quasiparticles that annihilate the new ground state $|z;\gamma\rangle$. The new quasiparticles are related to the old quasiparticles by a $c$-number shift

$$a_\nu=U_GA_\nu U_G^\dagger=A_\nu-z_\nu,\tag{36}$$

$$b=U_GBU_G^\dagger=B-\gamma.\tag{37}$$

To determine $z_\nu$ and $\gamma$, we rewrite the static part of $\mathscr{H}$, Eq. (30), in terms of new excitonic ($a_\nu$) and phononic ($b$) quasiparticle operators and force all linear terms ($\sim a_\nu$ and/or $\sim b$) to vanish. This procedure leads to a set of coupled nonlinear equations for the set of shift parameters ($\{z_\nu,\gamma\}$) and corresponds to mean-field equations of a *driven, weakly interacting two-component Bose gas*. With the previously described notation, the condition to make all linear parts vanish can be written in a very compact form

$$(\Omega_\nu-\omega_p)z_\nu+\sum_\mu\,[\Theta_{\nu\mu}+\Pi_{\nu\mu}+\Gamma_{\nu\mu}]z_\mu=\mu_\nu E_p,\tag{38}$$

$$\omega_0\gamma+\sum_{\nu,\mu}\,\mathscr{M}_{\nu\mu}z_\nu z_\mu=0,\tag{39}$$

where we used the fact that $z_\nu$ and $\gamma$ are real quantities. Here $\Theta$ is the Hartree self-energy due to exciton-exciton interaction, $\Pi$ due to (nonlinear) exciton-light interaction, and $\Gamma$ due to exciton-phonon interaction (lattice-relaxation energy). Explicitly, they are defined as

$$\Theta_{\nu\mu}=2\sum_{\lambda,\kappa}\,\mathscr{V}_{\nu\lambda\kappa\mu}z_\kappa z_\lambda,\tag{40}$$

$$\Pi_{\nu\mu}=3\sum_\lambda\,\tilde{\mu}_{\nu\mu\lambda}z_\lambda E_p,\tag{41}$$

$$\Gamma_{\nu\mu}=2.\mathscr{M}_{\nu\mu}\gamma,\tag{42}$$

where we used various symmetries of the interaction vertices Eqs. (31) and (33).

In physical terms, $z_\nu$ and $\gamma$ correspond to the pump-induced polarization and -stimulated phonons, respectively. More specifically, $n=\Sigma_\nu n_\nu=\Sigma_\nu|z_\nu|^2$ stands for the total pump-induced ($K=0$) exciton population, whereas $n_{\rm ph}=|\gamma|^2$ depicts the pump-stimulated population of ($Q=0$) optical phonons. For not too strong nonresonant pump fields the coupled set of mean-field equations can be solved iteratively. The ground state of the pumped EPG is then specified in terms of $z_\nu$ and $\gamma$. In Sec. III D we present numerical results for $n_\nu$ and $\gamma$ as a function of $\omega_p$ and Coulomb interaction strengths $U$ and $V$.

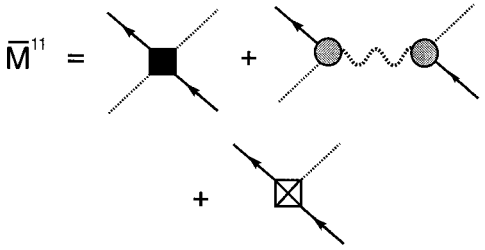

FIG. 6. Static part of the normal self-energy $\overline{M}^{11}$. The first and third diagrams are, respectively, due to exciton-exciton and (NL) exciton-light interactions. The second diagram depicts the phonon-mediated *static* exciton-exciton interaction.

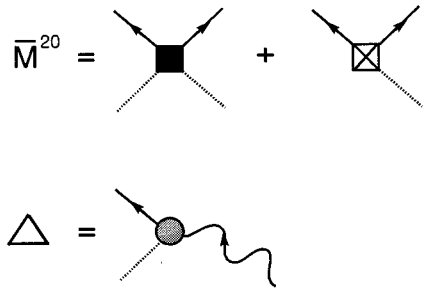

FIG. 7. Static part of the anomalous self-energy $\overline{M}^{20}$. The first diagram and the second diagram are due to exciton-exciton interaction and (NL) exciton-light interaction, respectively. $\Delta$ denotes the ''mixing of exciton and phonon degrees of freedom'' giving rise to the phonon-mediated *dynamic* exciton-exciton interaction.

### B. Collective excitations

We now calculate the excitation spectrum with respect to the coherent ground state of the pumped EPG employing the harmonic approximation, i.e., we rewrite the time-independent part of $\mathscr{H}$ in terms of shifted quasiparticles, Eqs. (36) and (37), and keep only terms that are at most bilinear in $a$ and $b$. Note that all linear terms vanish due to Eqs. (38) and (39). This is similar to the Bogoliubov approximation for the weakly interacting Bose gas.[36] Neglecting residual interaction terms (e.g., terms such as $\sim \mathscr{V} z a^\dagger a a$), the excitation spectrum of the pumped EPG is described by the quadratic form

$$\mathscr{H}_p^{(2)} = E(z;\gamma) + \sum_{\nu,\mu} \mathscr{A}_{\nu\mu} a_\nu^\dagger a_\mu + \omega_0 b^\dagger b + \frac{1}{2}\sum_{\nu,\mu} [\mathscr{B}_{\nu\mu} a_\nu^\dagger a_\mu^\dagger + \mathscr{B}_{\nu\mu} a_\nu a_\mu] + \sum_\nu [\Delta_\nu a_\nu^\dagger b^\dagger + \Delta_\nu a_\nu^\dagger b + \text{H.c.}]. \quad (43)$$

Here we attached a subscript $p$ to indicate that Eq. (43) describes the EPG in the presence of the pump laser and a superscript to denote the harmonic approximation. The $c$ number $E(z;\gamma)$ is the total ground-state energy of the pumped EPG. Since this energy does not show up in the optical response of the pumped system, we will not need the explicit form of $E(z;\gamma)$. It suffices to mention that it is obtained by replacing all exciton operators in the time-independent part of $\mathscr{H}$ by $z$ and all phonon operators by $\gamma$. We also introduced two real, symmetric $(N/2\times N/2)$ matrices **A** and **B** and a real $(N\times 1)$ matrix **Δ**

$$\mathscr{A}_{\nu\mu} = (\Omega_\nu - \omega_p)\delta_{\nu\mu} + \overline{\mathscr{M}}^{11}_{\nu\mu}, \quad (44)$$

$$\mathscr{B}_{\nu\mu} = 2\overline{\mathscr{M}}^{20}_{\nu\mu}, \quad (45)$$

$$\Delta_\nu = \sum_\mu \mathscr{M}_{\nu\mu} z_\mu. \quad (46)$$

The *static* part of the *normal* self-energy containing contributions from exciton-exciton, exciton-phonon, and (nonlinear) exciton-light interaction is given by

$$\overline{\mathscr{M}}^{11}_{\nu\mu} = \sum_{\kappa,\lambda} 4\mathscr{V}_{\nu\lambda\kappa\mu} z_\lambda z_\kappa + \sum_\lambda 2\mathscr{M}_{\nu\mu}\gamma + 4\tilde{\mu}_{\nu\lambda\mu} E_p z_\lambda \quad (47)$$

and describes scattering events between excitons residing in the condensate and excitons outside the condensate. To make the various contributions to the normal self-energy more transparent, we show graphically in Fig. 6 the various terms of Eq. (47). Black boxes stand for the exciton-exciton vertex and gray circles and boxes with a cross for exciton-phonon and exciton-pump interaction vertices, respectively. Solid straight and solid wavy lines represent, respectively, excitons and phonons above the condensate, whereas dashed straight and dashed wavy lines correspond to excitons and phonons residing in the condensate, respectively.

The *static* part of the *anomalous* self-energy comprising terms due to exciton-exciton and (nonlinear) exciton-light interaction reads

$$\overline{\mathscr{M}}^{20}_{\nu\mu} = \sum_{\kappa,\lambda} \mathscr{V}_{\nu\mu\lambda\kappa} z_\lambda z_\kappa + \sum_\lambda \tilde{\mu}_{\nu\lambda\mu} E_p z_\lambda \quad (48)$$

and describes spontaneous creation (annihilation) of excitons outside the condensate and thus fluctuations around the condensate. It is graphically depicted in the first part of Fig. 7. The physical meaning of $\Delta_\nu$ is that of a mixing amplitude between excitons and phonons outside the condensate giving rise to number-conserving as well as number-nonconserving processes. The scattering term is schematically depicted in the second part of Fig. 7. In contrast to the *static* phonon-mediated exciton-exciton interaction due to pump-stimulated phonons [the middle term in Eq. (47)], this contribution gives rise to a *dynamic*, i.e., resonant, interaction between excitons outside the condensate.

It is important to recall that within the harmonic approximation as specified by the *static* self-energies, Eqs. (47) and (48), multiple scattering of excitons is ignored. Thus it is not possible to consider biexciton formation. Furthermore, since there are many frequency-dependent *dynamic* self-energy diagrams that are also of $O(z^2)$ or $O(zE_p)$, the harmonic theory of (nonresonant) pump-and-probe spectroscopy is, similar to Bogoliubov's theory of a weakly interacting Bose gas, not completely consistent. Nevertheless, in the region near the optical gap, i.e., for $\omega_p + \omega_0 \sim \omega_t \sim \Omega_1$, it should give qualitatively correct results.

The bilinear form (43) can be diagonalized with a general Bogoliubov transformation[35] that amounts to the definition

of new *composite* quasiparticles. In terms of the new quasiparticle operator Eq. (43) reads

$$\mathscr{H}_p^{(2)}=\sum_j \epsilon_j d_j^\dagger d_j+E(z;\gamma)+\frac{1}{2}\left[\sum_j \epsilon_j-\sum_\nu \mathscr{A}_{\nu\nu}-\omega_0\right], \tag{49}$$

with the $N/2+1$ eigenenergies $\epsilon_j$ given by the solution of a nonsymmetric eigenvalue problem [of rank $2\times(N/2+1)$]

$$\begin{pmatrix} \mathscr{A} & \mathbf{\Delta} & \mathscr{B} & \mathbf{\Delta} \\ \widetilde{\Delta} & \omega_0 & \widetilde{\Delta} & 0 \\ \mathscr{B} & \mathbf{\Delta} & \mathscr{A} & \mathbf{\Delta} \\ \widetilde{\Delta} & 0 & \widetilde{\Delta} & \omega_0 \end{pmatrix} \begin{pmatrix} \mathscr{X}^j \\ V^j \\ \mathscr{Y}^j \\ W^j \end{pmatrix} = \epsilon_j \begin{pmatrix} \mathscr{T} & 0 & 0 & 0 \\ 0 & 1 & 0 & 0 \\ 0 & 0 & -\mathscr{T} & 0 \\ 0 & 0 & 0 & -1 \end{pmatrix} \times \begin{pmatrix} \mathscr{X}^j \\ V^j \\ \mathscr{Y}^j \\ W^j \end{pmatrix}. \tag{50}$$

The matrices $\mathscr{A}$ and $\mathscr{B}$ are defined in Eqs. (44) and (45), respectively, and $\widetilde{\Delta}$ is the transposite of $\mathbf{\Delta}$, given in Eq. (46). $\mathscr{X}^j$ and $\mathscr{Y}^j$ denote $N/2$ vectors, whereas $V^j$ and $W^j$ describe ordinary $c$ numbers. $\mathscr{T}$ stands for the $(N/2\times N/2)$ unit matrix and $\omega_0$ for the optical $(Q=0)$ phonon frequency.

The eigenmodes $(\mathscr{X},V,\mathscr{Y},W)$ of Eq. (50) describe the relation between the ''old'' and the ''new'' quasiparticles. Specifically, we find

$$a_\nu=\sum_j [\mathscr{X}_\nu^j d_j+\mathscr{Y}_\nu^j d_j^\dagger], \tag{51}$$

$$b=\sum_j [V^j d_j+W^j d_j^\dagger]. \tag{52}$$

From the inverse of Eqs. (51) and (52), it is clear that the eigenmodes $(\mathscr{X},V,\mathscr{Y},W)$, which depend on the pump parameters $\omega_p$ and $E_p$, determine the composition of the new excitations, i.e., phonon vs exciton contribution, and in turn their coupling to the test laser.

### C. Linear response

The full optical response of the pumped EPG contains not only absorption but also optical gain and is most conveniently obtained from general linear-response theory in terms of normal and anomalous (bosonized) exciton Green functions.[30] Here, however, we are interested only in the leading-order steady-state absorption spectrum of the EPG, which can be calculated with Fermi's golden rule.

We rewrite the time-dependent part of $\mathscr{H}$, Eq. (30), in terms of (Glauber-shifted) quasiparticles, i.e., $A\to a$. Keeping only terms linear in the new quasiparticles and calling all time-dependent terms of Eq. (30) $\mathscr{H}_t(t)$, we obtain, neglecting $c$-number contributions,

$$\begin{aligned}\mathscr{H}_t(t)=&-\sum_\nu \mu_\nu[1-f_\nu]a_\nu^\dagger \mathscr{E}_t e^{-i\Delta t} \\ &-\sum_\nu \mu_\nu[1-f_\nu]a_\nu \mathscr{E}_t e^{i\Delta t} \\ &+\sum_\nu \mu_\nu g_\nu a_\nu \mathscr{E}_t e^{-i\Delta t}+\sum_\nu \mu_\nu g_\nu a_\nu^\dagger \mathscr{E}_t e^{i\Delta t}.\end{aligned} \tag{53}$$

Here we defined correction factors $f_\nu$ and $g_\nu$, which come from the nonlinear exciton-light coupling and are explicitly given by

$$\begin{aligned}f_\nu=2g_\nu&=2\sum_{\mu,\lambda}\frac{\widetilde{\mu}_{\nu\mu\lambda}}{\mu_\nu}z_\mu z_\lambda \\ &=\frac{1}{2}\sum_l \sum_{\kappa,\mu,\lambda}\frac{\mu_\kappa}{\mu_\nu}\Phi^\kappa(l)\Phi^\nu(l)\Phi^\mu(l)\Phi^\lambda(l)z_\mu z_\lambda,\end{aligned} \tag{54}$$

where we used Eq. (33). $z_\nu$ is the pump-induced polarization obtained by a self-consistent solution of Eqs. (38) and (39). The product of exciton wave functions reflecting the internal structure of excitons is always smaller than one. Hence, for low pump intensities ($\sim|\mathscr{E}_p|^2$) and not too small detunings ($\Omega_1-\omega_p$), leading to $z_\nu<1$, we expect $f_\nu$ to be very small. All our numerical calculations have been made in this *weak-coupling regime*. Therefore, instead of considering the full (time-dependent) perturbation given in Eq. (53), we neglect all contributions $\sim f_\nu(g_\nu)$ and work approximately with

$$\mathscr{H}_t(t)\cong-\sum_\nu \mu_\nu\{a_\nu^\dagger \mathscr{E}_t e^{-i\Delta t}+\text{H.c.}\}. \tag{55}$$

In order to apply Fermi's golden rule, we rewrite Eq. (55) in terms of composite quasi-particles defined through the orthogonality transformation (51) and (52), which leads to

$$\mathscr{H}_t(t)=-\sum_{\nu,j}\{\mu_\nu[\mathscr{Y}_\nu^j d_j+\mathscr{X}_\nu^j d_j^\dagger]\mathscr{E}_t e^{-i\Delta t}+\text{H.c.}\}. \tag{56}$$

Furthermore, anticipating $\mathscr{Y}\ll\mathscr{X}$ and keeping only the resonant term $\sim e^{-i\Delta t}$, we finally get

$$\mathscr{H}_t(t)=-\sum_{\nu,j}\mu_\nu \mathscr{X}_\nu^j d_j^\dagger \mathscr{E}_t e^{-i\Delta t}. \tag{57}$$

We can now formally apply Fermi's golden rule to obtain for the (linear) absorption spectrum of the pumped EPG a very compact expression

$$\alpha(\omega)=8\pi^2 e^2\sum_j |f_j|^2\delta(\omega_t-\omega_p-\epsilon_j), \tag{58}$$

where $\omega_t$, $\omega_p$, and $\epsilon_j$ are, respectively, the frequency of the test laser, the pump frequency, and the excitation energies of the optically pumped EPG determined by the eigenvalue problem Eq. (50). The oscillator strength is given by

$$f_j=\sum_{\nu,l}\Phi^\nu(l)\mathscr{X}_\nu^j, \tag{59}$$

where we used definition (34) for the dipole matrix element $\mu_\nu$. In addition to the excitonic enhancement factor $\Phi^\nu$ there is now another oscillator strength renormalization $\mathscr{Z}^j$ due to pump-induced exciton-exciton, exciton-phonon, and (nonlinear) exciton-light interaction.

### D. Numerical results

We now present numerical results for the steady-state response of a coherently pump EPG in the collisionless regime with emphasis on the OSE and IRS. Specifically, we study a half-filled $N=160$ site system with periodic boundary conditions and two sets of model parameters. The first set, indicated in Table I, is representative for PDA (strong Coulomb interaction), whereas the second set is identical to the first one except for the Coulomb interaction, which is chosen to be $U=2V=0.4t_0$ (weak Coulomb interaction). With the first set of parameters, model (1) exhibits a strong (bound) exciton resonance at $\Omega_1=1.92$ eV that dominates the (linear) absorption spectrum and is comparable to the optical gap in polydiacetylene.[8] The exciton binding energy in this case is $\epsilon_b=0.675$ eV, which is larger than the optical phonon frequency $\omega_0=0.183$ eV. In contrast, the second set of parameters gives no bound exciton. In that case $\Omega_1=0.96$ eV and $\epsilon_b=0.02$ eV, comparable to the discreteness of energy levels due to finite-size effects and much smaller than the optical phonon frequency.

In both cases of a strong and a weak Coulomb interaction, we take for the pump field strength $\mathscr{E}_p=0.001$, which corresponds to a pump intensity of roughly $I_p=13$ MW/cm$^2$, a typical value for actual laser intensities in pump-and-probe spectroscopy. Keeping the pump field strength fixed, we vary the pump frequency $\omega_p$ and analyze pump-induced changes near the optical gap. In particular we consider pump and test frequencies such that $\omega_t\sim\Omega_1\sim\omega_p+\omega_0$. In the following we measure energies in units of $2t_0$ and, introducing a parameter $\Theta=(\Omega_1-\omega_p)/\omega_0$, the detuning of the pump frequency from the optical gap in units of $\omega_0$.

First, we consider the coherent ground state of the pumped EPG. An iterative solution of the mean-field equations, Eqs. (38) and (39), gives numerical data for the pump-induced polarization $z_\nu$ and stimulated phonons $\gamma$. Figure 8 shows the corresponding pump-induced exciton population $n_\nu=|z_\nu|^2$ for a strong and a weak Coulomb interaction in semilogarithmic scale for $\Theta=1$. Clearly, in the case of a strong Coulomb interaction the bound exciton state ($\nu=1$) is much more populated than the scattering states ($\nu\geqslant 2$), i.e., $n_1\gg n_\nu$ for $\nu\geqslant 2$. For a weak Coulomb interaction the lowest state is no longer as distinct and the distribution of $n_\nu$ is much smoother; nevertheless, the lowest states do still dominate. In our calculations of the steady-state response of the pumped EPG, we kept the whole two-particle spectrum, which is consistent with our assumption of ultrashort pulses with a width much smaller than intrinsic relaxation times. We point out that even for *resonant* excitation with ultrashort pulses it is not possible to ignore scattering states and restrict the theory to an effective few-level system, e.g., ground state and exciton. This has been nicely demonstrated experimentally using time-resolved FWM in quantum wells.[37]

In Fig. 9 we show the population of the lowest exciton state as a function of $\Theta$ for strong and weak Coulomb interactions. The *excitonic enhancement* of the occupancy of the lowest state can be clearly seen. Finally, Fig. 10 shows $\gamma$ as a function of $\Theta$. It is obvious from Figs. 9 and 10 that, only for $\Theta\sim 1$, i.e., $\omega_p\sim\Omega_1-\omega_0$, there is a considerable amount of stimulated excitons and phonons. Both consitute a *coherent condensate* whose excitations in turn are measured by the second weak test field.

Employing a Ullah-Rowe algorithm,[38] the eigenvalue problem Eq. (50) can be straightforwardly solved and gives the excitation spectrum of the pumped EPG. These excitations are *composite quasiparticles* whose phononic and excitonic degrees of freedom depend on pump parameters. Moreover, since light couples exclusively to the excitonic component, we expect that the oscillator strength associated with these quasiparticles also varies significantly with $\omega_p$ and $\mathscr{E}_p$. This is demonstrated in Fig. 11, which depicts, for the strong Coulomb interaction alone, the normalized oscillator strength for the two lowest excitations of the pumped EPG. For $\Theta\sim 1$, the lowest excitation of the pumped EPG becomes ''brighter,'' i.e., with increasing oscillator strength, whereas the next highest excitation loses oscillator strength. In Fig. 12 we depict the energetic position of these resonances as a function of $\Theta$. For large $\Theta$, i.e., large detuning, the lowest resonance closely follows $\omega_p+\omega_0=\Omega_1-(\Theta-1)\omega_0$, indicating its phononic precursor and its connection to IRS.[39] The second resonance starts out from the bare exciton energy $\Omega_1$ and begins to deviate from that value as $\Theta$ approaches 1 (see Fig. 13). From Figs. 11, 12, and especially Fig. 13 we see that for $\Theta\sim 1$, the excitations of the optically pumped EPG are significantly modified compared to the excitations of the unperturbed EPG. In other words, pump photons with frequency $\omega_p=\Omega_1-\omega_0$ start to initiate a strong mixing, i.e., renormalization, of the bare quasiparticles, optical phonon, and TDA exciton.

Experimentally, strong renormalization effects can be seen in the differential absorption spectrum as a function of temporal delay between (finite) pump and test pulses. Since we take into account neither the finite width of the laser pulses nor the delay between pump and test pulses, a sound calculation of the *differential absorption spectrum* is outside our simplified Hamiltonian theory for the steady-state response of the pumped EPG. As a crude approximation we can, however, study the *difference absorption spectrum*, i.e., absorption of the test laser field with the pump field *on* minus the test beam absorption with the pump laser *off*. Although [Eq. (58) with Lorentzian broadening of 0.001] not quite accurate, it should give at least a qualitative picture for the differential absorption spectrum at zero time delay and pulses much shorter than intrinsic relaxation times (see Sec. III A). Figures 14 and 15 show, for the case of a strong and a weak Coulomb interaction, respectively, the difference absorption near the optical gap of the unperturbed EPG, i.e., $\omega_t\sim\Omega_1$, for various values of $\Theta$. The peak at the high-energy side originates from the shifted exciton resonance (i.e., OSE), whereas the signature at the low-energy side depicts the appearance of the IRS resonance. As is also the case in atomic physics,[39] the line shape of the IRS resonance strongly depends on the pump frequency, i.e., on $\theta$. This is due primarily to the interference of the OSE with the IRS and can be clearly seen in both Figs. 14 and 15. For instance, in Fig. 14 the shape of the IRS signal (low-energy feature) changes from absorptive $\Theta=1.12$ to dispersive $\Theta=1.0$ to

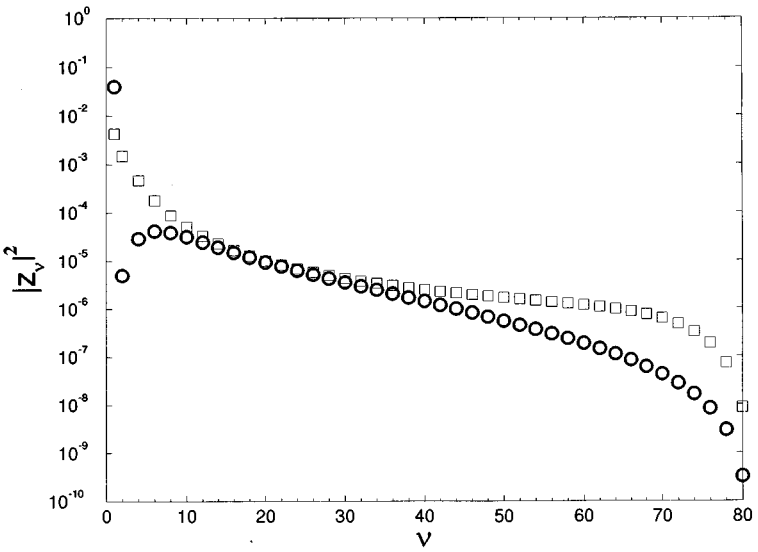


FIG. 8. Pump-induced population of optically active excitons for $\Theta = 1$. Circles denote the case of a strong Coulomb interaction, while squares depict the case of a weak Coulomb interaction.

transmissive $\Theta = 0.96$ and back to dispersive $\Theta = 0.88$. Similar changes, although less pronounced, occur for the case of weak Coulomb interaction, Fig. 15. The qualitative change of the IRS line shape has been experimentally observed by Blanchard *et al.*[4,9]

Our primary objective is to provide a *microscopic understanding* of pump-and-probe spectroscopy. Therefore, we now address the question as to what extent the various interactions, such as exciton-exciton, exciton-phonon, and (nonlinear) exciton-light coupling, give rise to renormalization of the quasiparticles of the pumped EPG. In Figs. 16 and 17 we depict for $\Theta = 1$ and both cases of strong and weak Coulomb interaction how the difference absorption spectrum would look if we had kept as nonlinearities only (i) the exciton-exciton, (ii) the exciton-phonon, or (iii) the (nonlinear) exciton-light interaction alone. Both Figs. 16 and 17 show that the (nonlinear) exciton-light interaction only slightly renormalizes the excitation spectrum of the pumped EPG resulting in a small blueshift of the optical gap. In contrast, the exciton-exciton interaction causes a large blueshift, indicating a significant effect on the excitations of the pumped EPG. Obviously, the stronger the original Coulomb interaction, the stronger this effect. The exciton-phonon interaction gives rise in both cases to a double-peak structure due to the IRS resonance and shifted optical gap. Comparing the full response (all interaction processes taken together) for strong and weak Coulomb interactions, respectively, we see that the double-peak structure persists, although in the case of the strong Coulomb interaction a significant redistribution of oscillator strength occurs; the ''phononic'' part of the double-peak structure is less pronouced in the case of a strong Coulomb interaction.

Thus, within our simplified theory, neglecting transient aspects of the light-matter coupling (delay, pulse shapes), it is exclusively the relative strength of the Coulomb and the electron-phonon interaction giving rise to *static* exciton-exciton, exciton-phonon, and (nonlinear) exciton-light coupling, which controls, for fixed detuning $\Theta$ and pump intensity $I_p \sim |\mathscr{E}_p|^2$, the excitation spectrum of the pumped EPG and hence the shape of the difference spectrum. As far as measured differential absorption spectra are concerned, it is, however, the *dynamic* weighting of these interactions due to transient aspects, such as impulsive laser excitation and temporal delay between the pump and test pulses, that strongly affects the observed line shapes.

## IV. CONCLUSION

We have proposed, following the seminal work of Schmitt-Rink, Chemla, and Haug,[14] an alternative description of nonlinear optics of conjugated polymers in terms of an externally driven EPG, i.e., a two-component Bose gas, emphasizing throughout the paper the importance of (i) exciton-exciton, (ii) exciton-phonon, and (iii) (nonlinear) exciton-light coupling. Starting from a model for interacting $\pi$ electrons coupled to a one-dimensional lattice, we utilized the Sakamoto-Kishimoto boson expansion technique[12] and presented a detailed and transparent derivation of an effective EPG Hamiltonian based on (one-dimensional) TDA excitons calculated with respect to the Peierls-dimerized ground state. We gave expressions for the interaction vertices and employed mode-mode coupling diagrams to visualize the physics content. The harmonic-oscillator interpretation of nonlinear optics effects, or, equivalently, the boson

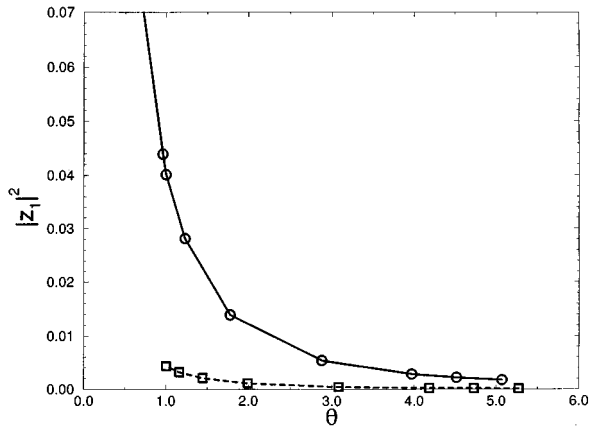


FIG. 9. Pump-induced population of the lowest exciton state. Circles denote the case of a strong Coulomb interaction (bound particle-hole pair), while squares stand for a weak Coulomb interaction (no bound state).

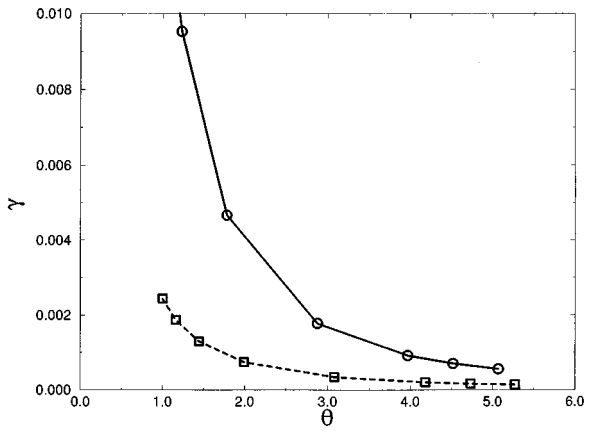


FIG. 10. Stimulated optical phonons. Circles denote the case of a strong Coulomb interaction, while squares stand for a weak Coulomb interaction.

representation chosen in this paper, dates back to the beginning of nonlinear optics.[40] It is, however, only recently in the field of conjugated polymers that such an approach has been applied.[41] Although the authors of Ref. 41 do not explicitly introduce a bosonic quasiparticle description for the electronic subsystem, there are, nevertheless, similarities to our approach, which is not surprising since both approaches are from a technical point of view perturbative extensions of standard harmonic approximations: the TDA in our case and the random-phase approximation (RPA) in Ref. 41.

The discussion of pump-and-probe spectroscopy was restricted to the steady-state response of a coherently pumped EPG in the collisionless regime. Specifically, we explained the OSE and IRS in terms of *composite excitations* whose excitonic and phononic degrees of freedom are determined by the parameter of the pump laser, i.e., pump frequency and pump intensity. Except for the classical treatment of the light field, these composite quasiparticles are related to *phonoritons* introduced in Ref. 42 to study similar effects in inorganic (bulk) semiconductors. We showed how Coulomb interactions affect the coherent optical response and discussed the relative importance of various interaction processes on the excitation spectrum of the pumped EPG and hence on the

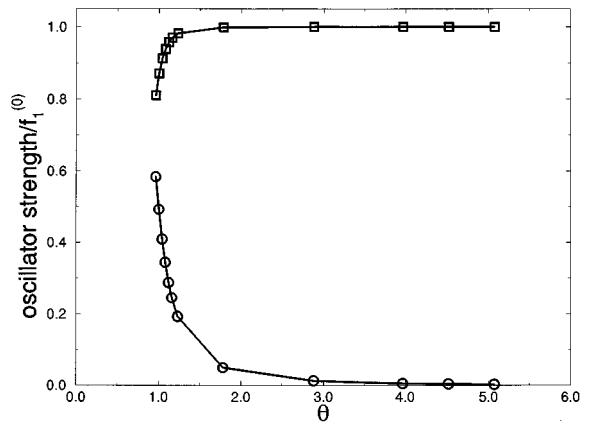


FIG. 11. Normalized oscillator strength of the two lowest excitations of the pumped EPG. Circles denote the IRS resonance (lowest excitation), while squares depict the shifted optical gap (OSE).

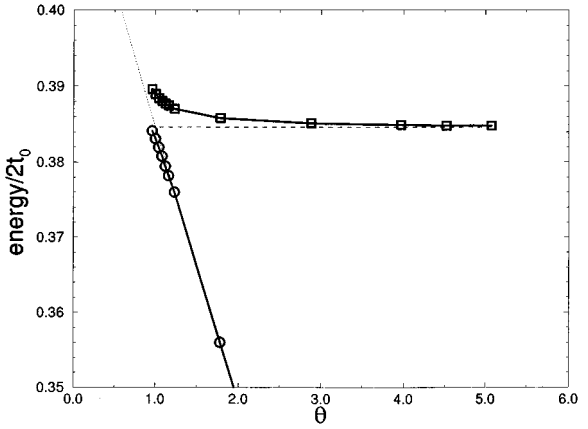


FIG. 12. Energetic position of the two lowest excitations of the pumped EPG. Circles denote the IRS resonance (lowest excitation), while squares depict the shifted optical gap (OSE). Dotted and dashed lines stand for $\omega_p+\omega_0$ and $\Omega_1$, respectively.

difference absorption spectrum $\Delta\alpha$.

For a detailed comparison with experiments our EPG approach is not yet developed completely enough, and in contrast to phenomenological multimode Brownian oscillator models,[43] we are not yet able to reproduce all experimental features. One drawback of these phenomenological models is, however, that they do not clarify the underlying many-body processes and are in this sense *ad hoc*. We, on the other hand, are able to determine the consequences of various many-body effects on the excitation spectrum of the pumped conjugated polymer and to give a *microscopic understanding* of the underlying physics in terms of (renormalized) quasiparticles. For a more advanced treatment of pump-and-probe spectroscopy we should solve, however, the full externally driven Beliaev equations for the normal and anomalous exciton Green functions,[30] taking finite pulse shapes, delays, and possibly also *dynamic* self-energies due to higher-order correlations of the coupled EPG into account. The latter is important for a treatment of the driven EPG beyond the mean field approximation, for instance, to take correlations between excitons into account. Conjugated polymers are

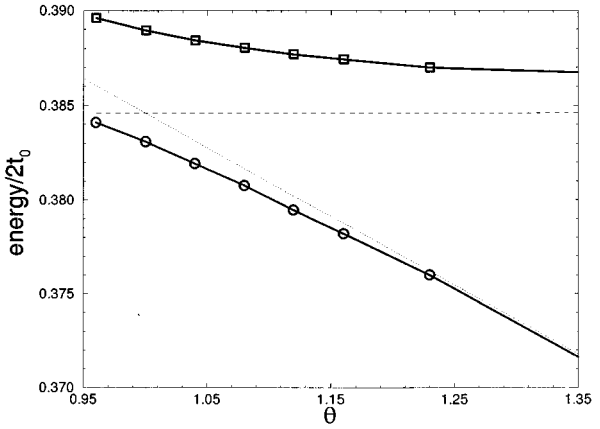


FIG. 13. Energetic position of the two lowest excitations of the pumped EPG for $\Theta\sim 1$. Circles denote the IRS resonance (lowest excitation), while squares depict the shifted optical gap (OSE). Dotted and dashed lines stand for $\omega_p+\omega_0$ and $\Omega_1$, respectively.

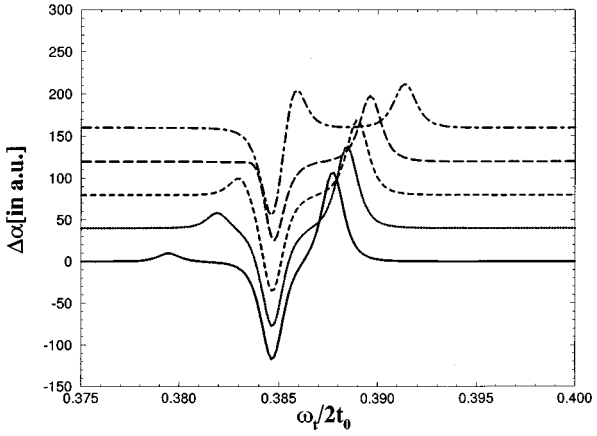


FIG. 14. Difference absorption spectrum near the optical gap for the case of strong Coulomb interactions and various values of pump detuning $\Theta$: $\Theta=1.12$ (solid line), $\Theta=1.04$ (dotted line), $\Theta=1.0$ (dashed line), $\Theta=0.96$ (long-dashed line), and $\Theta=0.88$ (dot-dashed line). The curves are artifically shifted on the vertical axis.

wide-gap semiconductors and it is conceivable that for a sufficiently strong Coulomb interaction biexcitons and perhaps even higher-order bound complexes — so-called $n$ strings[44] — stabilized by low dimensionality can be formed. To take biexciton formations into account and to study their signatures in nonlinear spectroscopy, e.g., in two-photon absorption, it is required to calculate the $T$ matrix for mutiple-exciton scattering, which indeed gives rise to frequency-dependent, i.e., dynamic, self-energies. Another important issue for the photophysics of low-dimensional conjugated polymers is disorder due to electronic and/or mechanic imperfections arising in the course of the synthesis or due to deliberate doping and/or blending of polymers. Especially due to the Q1D nature of these materials, it is expected that for a complete microscopic understanding of transient spectroscopy it is necessary to treat disorder not only in the lowest approximation, e.g., Born approximation, giving rise to decay rates, but to higher order where disorder induces localized states. Whether an exciton localizes as a whole or breaks up into its constituents, a particle and a hole, which then in turn localize individually, is an open question and deserves, also from a fundamental point of view, more attention. We hope that the EPG approach presented can be utilized to shed light on this interesting problem.

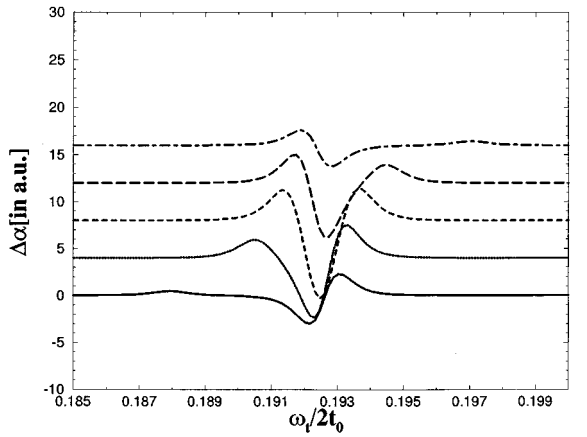


FIG. 15. Difference absorption spectrum near the optical gap for the case of weak Coulomb interactions and various values of pump detuning $\Theta$: $\Theta=1.12$ (solid line), $\Theta=1.04$ (dotted line), $\Theta=1.0$ (dashed line), $\Theta=0.96$ (long-dashed line), and $\Theta=0.88$ (dot-dashed line). The curves are artifically shifted on the vertical axis.

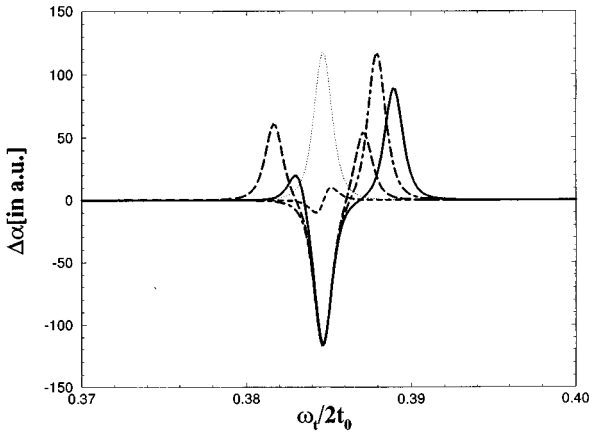


FIG. 16. Difference absorption spectrum for the case of a strong Coulomb interaction and $\Theta=1$ as obtained by considering (i) exciton-exciton (dot-dashed line), (ii) (nonlinear) exciton-light (dashed line), and (iii) excition-phonon interactions (long-dashed line) separately. The solid line depicts the complete $\Delta\alpha$ with all interaction processes taken into account. For reference, we also show the unperturbed exciton line (dotted).

## APPENDIX A: MEAN-FIELD APPROXIMATION

Following Hayashi and Nasu,[16] the mean-field approximation for model (1) consists of (i) an unrestricted Hartree-Fock approximation for the Coulomb interaction and (ii) a Born-Oppenheimer approximation for the electron-lattice coupling. First, it is convenient to define a dimensionless lattice field

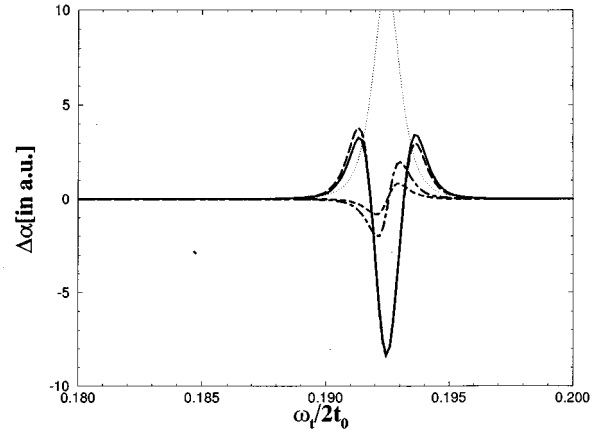


FIG. 17. Difference absorption spectrum for the case of a weak Coulomb interaction and $\Theta=1$ as obtained by considering (i) exciton-exciton (dot-dashed line), (ii) (nonlinear) exciton-light (dashed line), and (iii) exciton-phonon interactions (long-dashed line) separately. The solid line depicts the complete $\Delta\alpha$ with all interaction processes taken into account. For reference, we also show the unperturbed exciton line (dotted line).

$$q_l=\frac{K}{2\alpha}u_l, \tag{A1}$$

together with dimensionless coupling constants $u=U/2t_0$, $v=V/2t_0$, and $\lambda=2\alpha^2/Kt_0$ and a dimensionless lattice mass (adiabaticity parameter) $\delta=\lambda/(\omega_0/2t_0)^2$, which allows us to measure energies in units of $2t_0$, i.e., $H\rightarrow H/2t_0$. Anticipating the BOW (Peierls-dimerized) ground state, we divide the (dimensionless) lattice field into a static part (dimerization) and a dynamic part (phonons)

$$q_l(t)=q(-)^l+\chi_l(t) \tag{A2}$$

and write for the charge ($n_{l\sigma}=c^\dagger_{l\sigma}c_{l\sigma}$) and bond ($m_{l\sigma}=c^\dagger_{l\sigma}c_{l+1\sigma}$) densities (anticipating half filling and again the Peierls instability)

$$\langle n_{l\sigma}\rangle=\frac{1}{2}, \tag{A3}$$

$$\langle m_{l\sigma}\rangle=\langle m^\dagger_{l\sigma}\rangle=\overline{m}+(-1)^l\delta m. \tag{A4}$$

The three parameter $\overline{m}$, $\delta m$, and $q$, related to bandwidth renormalization and to the single-particle gap, will be determined self-consistently at the end of this appendix. Using the well-known operator identity

$$\hat{A}\hat{B}=\hat{A}\langle\hat{B}\rangle+\hat{B}\langle\hat{A}\rangle-\langle\hat{A}\rangle\langle\hat{B}\rangle+[\hat{A}-\langle\hat{A}\rangle][\hat{B}-\langle\hat{B}\rangle] \tag{A5}$$

to decouple an effective single-particle part from an explicit two-body contribution, we regroup Eq. (1) into

$$H=H_{\rm MF}+H^0_{\rm ph}+\delta H_{e\text{-}e}+\delta H_{e\text{-ph}}. \tag{A6}$$

Here $H_{\rm MF}$ and $H^0_{\rm ph}$ denote, respectively, the electronic and the phononic one-body part, whereas $\delta H_{e-e}$ and $\delta H_{e-{\rm ph}}$ depict two-body terms due to (residual) electron-electron and electron-phonon interactions. Furthermore, we define in the *extended BZ*, i.e., $-\pi\leqslant k<\pi$, electronic operators (unit lattice constant)

$$c_{k\sigma}=\frac{1}{\sqrt{N}}\sum_l e^{-ikl}c_{l\sigma} \tag{A7}$$

and phonon operators

$$\chi_l=\frac{1}{\sqrt{N}}\sum_q e^{iql}\sqrt{\frac{1}{2\delta\omega(q)}}[b_q+b^\dagger_{-q}]. \tag{A8}$$

Specifically in momentum space, we then obtain in the *reduced BZ*, i.e., $-\pi/2\leqslant k<\pi/2$ (doubling of the unit cell due to Peierls instability), for the electronic single-particle part,

$$H_{\rm MF}=\overline{H}+\sum_{k,\sigma}[\epsilon_k(c^\dagger_{k\pm\pi\sigma}c_{k\pm\pi\sigma}-c^\dagger_{k\sigma}c_{k\sigma})+i\Delta_k(c^\dagger_{k\pm\pi\sigma}c_{k\sigma}-c^\dagger_{k\sigma}c_{k\pm\pi\sigma})], \tag{A9}$$

with

$$\epsilon_k=2\tilde{t}_0\cos k, \tag{A10}$$

$$\Delta_k=4\tilde{\alpha}\tilde{u}\sin k, \tag{A11}$$

and

$$\tilde{t}_0=\frac{1}{2}+v\overline{m}, \tag{A12}$$

$$2\tilde{\alpha}\tilde{u}=\lambda q+v\,\delta m, \tag{A13}$$

$$\overline{H}=N\left[\frac{u}{4}+v+2v(\overline{m^2}+\delta m^2)+2\lambda q^2\right]. \tag{A14}$$

In the extended BZ, the free phonon part becomes

$$H^0_{\rm ph}=\sum_q\left[\omega(q)b^\dagger_q b_q+\frac{1}{2}\right], \tag{A15}$$

whereas in the reduced BZ, introducing acoustic- ($b_{1q}=b_q$) and optic- ($b_{2q}=b_{q\pm\pi}$) phonon operators, it reads

$$H^0_{\rm ph}=\sum_{\lambda,q}\omega_\lambda(q)\left[b^\dagger_{q\lambda}b_{q\lambda}+\frac{1}{2}\right], \tag{A16}$$

with acoustic- and optic-phonon branches given, respectively, by

$$\omega_1(q)=\sqrt{\frac{4\lambda}{\delta}}\left|\sin\frac{q}{2}\right|, \tag{A17}$$

$$\omega_2(q)=\sqrt{\frac{4\lambda}{\delta}}\cos\frac{q}{2}. \tag{A18}$$

Residual electron-electron and electron-phonon interactions read, in the extended BZ (: : denote normal ordering),

$$\delta H_{e\text{-}e}=\frac{1}{2N}\sum_{k_1,k_2,k_3,k_4,\sigma,\tau}u(k_1-k_4):c^\dagger_{k_1\sigma}c^\dagger_{k_2\tau}c_{k_3\tau}c_{k_4\sigma}:, \tag{A19}$$

$$\delta H_{e\text{-ph}}=\sum_{k_1,k_2,q}g(k_1,k_2,q)[b_q+b^\dagger_{-q}]:c^\dagger_{k_1\sigma}c_{k_2\sigma}:, \tag{A20}$$

with interaction vertices defined in momentum space

$$u(q)=u+2v\cos(q), \tag{A21}$$

$$g(k_1,k_2,q)=i\lambda\sqrt{\frac{1}{2\delta\omega(q)N}}[\sin k_1-\sin k_2]. \tag{A22}$$

Due to translational invariance the momentum summations in Eqs. (A19) and (A20) are, respectively, restricted to $k_1+k_2=k_3+k_4$ and $k_1-k_2=q$. In Appendix B we eventually work out expressions for (A19) and (A20) in the reduced BZ. The phonon dispersion in Eq. (A22) has the form given in Eq. (A17); note, however, that $q$ in Eq. (A20) covers the extended BZ.

The (bilinear) single-particle Hamiltonian $H_{\rm MF}$ is diagonalized by a Bogoliubov transformation specifying new mean-field quasiparticles $a_{k\sigma\pm}$ related to bare electrons via

$$c_{k\sigma}=\alpha_k a_{k\sigma-}+\beta_k a_{k\sigma+}, \tag{A23}$$

$$c_{k\pm\pi\sigma}=-i\beta_k a_{k\sigma-}+i\alpha_k a_{k\sigma+}. \tag{A24}$$

In terms of quasiparticle operators, we find

$$H_{\mathrm{MF}}=\sum_{k,\sigma} E_k[a^{\dagger}_{k\sigma+}a_{k\sigma+}-a^{\dagger}_{k\sigma-}a_{k\sigma-}]+\overline{H}, \quad \text{(A25)}$$

with the MFA dispersion given by

$$E_k=\sqrt{[(1+2v\overline{m})\cos k]^2+[(2\lambda q+2v\,\delta m)\sin k]^2} \quad \text{(A26)}$$

and the BOW ground state written as

$$|\mathscr{M}\rangle=\Pi_{k\sigma}a^{\dagger}_{k\sigma-}|0\rangle. \quad \text{(A27)}$$

The phonon part of $|\mathscr{M}\rangle$ corresponds to the vacuum of $b_q$ and is included in $|0\rangle$, which is also the vacuum for the bare electrons. To make the analogy with semiconductors as transparent as possible, we now define in the reduced BZ particle and hole operators

$$p_{k\sigma}=a_{k\sigma+}, \quad \text{(A28)}$$

$$h_{k\sigma}=a^{\dagger}_{-k\bar{\sigma}-} \quad \text{(A29)}$$

and finally obtain for the electronic single-particle Hamiltonian

$$H_{\mathrm{MF}}=\sum_{k,\sigma} E_k[p^{\dagger}_{k\sigma}p_{k\sigma}+h^{\dagger}_{k\sigma}h_{k\sigma}]+E_{\mathrm{MFA}}. \quad \text{(A30)}$$

Using Eq. (A14) the total MFA ground-state energy is given by

$$E_{\mathrm{MFA}}=-\sum_{k,\sigma} E_k+N\left[\frac{u}{4}+v+2v(\overline{m^2}+\delta m^2)+2\lambda q^2\right]. \quad \text{(A31)}$$

The three parameter $\overline{m}$, $\delta m$, and $q$, which, in fact, are only two since $\delta m=q$ in the BOW phase, are determined from a set of coupled nonlinear self-consistency equations involving complete elliptic integrals of the first (**K**) and the second (**E**) kind.[16] In our notation the set of self-consistency equations read[30]

$$c=\frac{2\mu c(\lambda+v)}{\pi(\mu^2-c^2)}[\mathbf{K}(y)-\mathbf{E}(y)], \quad \text{(A32)}$$

$$\mu=\frac{2\mu^2 v}{\pi(\mu^2-c^2)}\left[\mathbf{E}(y)-\left(\frac{c}{\mu}\right)^2\mathbf{K}(y)\right]+1, \quad \text{(A33)}$$

with $c=2(\lambda+v)q$, $\mu=1+2v\overline{m}$, and $y=\sqrt{1-(c/\mu)^2}$. In terms of $c$ and $\mu$ the mean-field single-particle gap separating at half filling the full valence from the empty conduction band and the renormalized bandwidth are given, respectively, by $E_{\mathrm{gap}}=2E_{\pi/2}=2c$ and $W_{\mathrm{band}}=2E_0=2\mu$. To obtain quantitative results for $E_{\mathrm{gap}}$ and $W_{\mathrm{band}}$, we solve the coupled set of nonlinear equations (A32) and (A33) numerically. For later reference, we conclude this appendix with explicit expressions for the Bogoliubov amplitudes

$$\alpha_k=\sqrt{\frac{E_k+\epsilon_k}{2E_k}}, \quad \text{(A34)}$$

$$\beta_k=\sqrt{\frac{E_k-\epsilon_k}{2E_k}}\,\mathrm{sgn}(k), \quad \text{(A35)}$$

with $\epsilon_k$ and $E_k$ defined in Eqs. (A10) and (A26), respectively.

## APPENDIX B: PARTICLE-HOLE REPRESENTATION

Because our notations are somewhat different from Ref. 16 and also to make clear what kind of processes are left out in Eq. (4), we briefly recall the transformation of model (1) into particle-hole representation. First, we consider the residual electron-electron interaction

$$\delta H_{e\text{-}e}=\frac{1}{2N}\sum_{k_1,k_2,k_3,k_4,\sigma,\tau} u(k_1-k_4):c^{\dagger}_{k_1\sigma}c^{\dagger}_{k_2\tau}c_{k_3\tau}c_{k_4\sigma}:, \quad \text{(B1)}$$

with $u(q)$ defined in Eq. (A21) and momentum sums over the extended BZ, i.e., $-\pi\leqslant k<\pi$, and restricted by $k_1+k_2=k_3+k_4$. We regroup Eq. (B1) into

$$\delta H_{e\text{-}e}=\delta H^{\mathrm{TDA}}_{e\text{-}e}+\delta H^{\mathrm{RPA}}_{e\text{-}e}+\delta H^{pp}_{e\text{-}e}+\delta H^{hh}_{e\text{-}e}+\delta\widetilde{H}_{e\text{-}e}. \quad \text{(B2)}$$

The physical meaning of the various terms is as follows. The first term denotes scattering of particle-hole pairs and consists of a direct and an exchange term. The second term describes the spontaneous creation and annihilation of particle-hole pairs leading to RPA correlations, whereas the next two terms stand for the mutual interaction of particles in the conduction band and holes in the valence band, respectively. Finally, the last term contains all remaining processes for which we do not give explicit expressions.

In the reduced BZ, i.e., $-\pi/2\leqslant k<\pi/2$, Eq. (B1) leads to 81 terms. To keep the Hamiltonian as simple as possible, we retain only those terms which are important for optical processes. In particular we disregard all umklapp processes ($U$ processes) with respect to the reduced BZ, i.e., processes for which momentum is conserved only up to a multiple of $\pi$ (reciprocal lattice vector of the dimerized lattice). Furthermore, we ignore all terms that describe the scattering of a particle (hole) via creating or annihilating a particle-hole pair, e.g., terms $\approx p^{\dagger}_{k_1\sigma}p^{\dagger}_{k_2\tau}\,p_{k_3\tau}\,h^{\dagger}_{k_4\sigma}$. These type of processes gives rise to a polarization of electronic orbitals and can be taken into account by a proper dielectric constant.[21,22] Separating the processes retained in the way indicated in Eq. (B2), we obtain, in the reduced BZ,

$$\delta H^{\mathrm{TDA}}_{e\text{-}e}=-\frac{1}{N}\sum_{k_i,\sigma,\tau} V^{eh,d}_{1234}\,p^{\dagger}_{k_2\tau}h^{\dagger}_{-k_4\sigma}h_{-k_1\bar{\sigma}}p_{k_3\tau}+\frac{1}{N}\sum_{k_i,\sigma,\tau} V^{eh,x}_{1234}\,p^{\dagger}_{k_2\tau}h^{\dagger}_{-k_3\tau}h_{-k_1\bar{\sigma}}p_{k_4\sigma}, \quad \text{(B3)}$$

$$\delta H^{\mathrm{RPA}}_{e\text{-}e}=\frac{1}{2N}\sum_{k_i,\sigma,\tau}[V^{\mathrm{RPA}}_{1234}\,p^{\dagger}_{k_1\sigma}p^{\dagger}_{k_2\tau}\,h^{\dagger}_{-k_3\tau}h^{\dagger}_{-k_4\bar{\sigma}}+\mathrm{H.c.}], \quad \text{(B4)}$$

$$\delta H^{pp}_{e\text{-}e}=\frac{1}{2N}\sum_{k_i,\sigma,\tau} V^{pp}_{1234}\,p^{\dagger}_{k_1\sigma}p^{\dagger}_{k_2\tau}\,p_{k_3\tau}p_{k_4\sigma}, \quad \text{(B5)}$$

$$\delta H^{hh}_{e\text{-}e}=\frac{1}{2N}\sum_{k_i,\sigma,\tau} V^{hh}_{1234}h^{\dagger}_{-k_3\tau}h^{\dagger}_{-k_4\bar{\sigma}}h_{-k_1\bar{\sigma}}h_{-k_2\bar{\tau}} \quad \text{(B6)}$$

where, as before, the momentum summation is constrained to $k_1+k_2=k_3+k_4$. The interaction vertices are given by

$$V^{eh,d}_{1234}=u\Phi_{1234}-2v\Psi_{1234}\cos(k_1-k_4), \tag{B7}$$

$$V^{eh,x}_{1234}=u\Phi_{1234}+2v\Psi_{1234}\cos(k_1-k_4), \tag{B8}$$

$$V^{\mathrm{RPA}}_{1234}=-u\Phi_{1234}-2v\Psi_{1234}\cos(k_1-k_4), \tag{B9}$$

$$V^{pp}_{1234}=u\Phi_{1234}-2v\Psi_{1234}\cos(k_1-k_4), \tag{B10}$$

$$V^{hh}_{1234}=u\Phi_{1234}-2v\Psi_{1234}\cos(k_1-k_4). \tag{B11}$$

Here numerical indices stand for momentum variables, e.g.,

$$V^{()}_{1234}\rightarrow V(k_1,k_2,k_3,k_4)^{()}, \tag{B12}$$

and we employed auxiliary functions

$$\Phi_{1234}=f^{+}_{12}f^{+}_{34}+g^{-}_{12}g^{-}_{34}, \tag{B13}$$

$$\Psi_{1234}=f^{-}_{12}f^{-}_{34}-g^{+}_{12}g^{+}_{34}, \tag{B14}$$

together with

$$f^{\pm}_{12}=\alpha_1\beta_2\pm\beta_1\alpha_2, \tag{B15}$$

$$g^{\pm}_{12}=\alpha_1\alpha_2\pm\beta_1\beta_2, \tag{B16}$$

where $\alpha_1$ and $\beta_1$ are Bogoliubov amplitudes defining MFA quasiparticles as given in Appendix A, Eqs. (A34) and (A35). Expressions (B3)–(B6) are identical to the ones given in Ref. 16, except with slighly different notations. Since spontaneous creation or annihilation of particle-hole pairs is suppressed due to the presence of a single-particle gap ($\sim$2 eV in PDA), we do not consider $\delta H^{\mathrm{RPA}}_{e-e}$ in the main text. A bosonization technique based on RPA collective pairs is possible, although it is algebraically much more involved.[45]

Let us now turn to residual electron-phonon interaction. For completeness we give the full expression (except $U$ processes) including intraband and interband scattering events as well as optic and acoustic phonons. In the main part of the paper, however, we consider only intraband scattering of optic phonons. In the reduced BZ we split Eq. (A20) into intra- and interband processes

$$\delta H_{e\text{-ph}}=\delta H^{\mathrm{intra}}_{e\text{-ph}}+\delta H^{\mathrm{inter}}_{e\text{-ph}}. \tag{B17}$$

Neglecting umklapp scattering with respect to the reduced BZ and using acoustic- (optic-) phonon operators (see Appendix A) we explicitly find

$$\delta H^{\mathrm{intra}}_{e\text{-ph}}=\sum_{j=1,2}\sum_{k_1,k_2,q}\sum_{\sigma} W^{\mathrm{intra}}_j(k_1,k_2,q)[p^{\dagger}_{k_1\sigma}p_{k_2\sigma} + h^{\dagger}_{-k_2\sigma}h_{-k_1\sigma}](b_{qj}+b^{\dagger}_{-qj}), \tag{B18}$$

$$\delta H^{\mathrm{inter}}_{e\text{-ph}}=\sum_{j=1,2}\sum_{k_1,k_2,q}\sum_{\sigma}[W^{\mathrm{inter}}_j(k_1,k_2,q) \times p^{\dagger}_{k_1\sigma}h^{\dagger}_{-k_2\sigma}(b_{qj}+b^{\dagger}_{-qj})+\mathrm{H.c.}], \tag{B19}$$

where the momentum sums are restricted to $k_1-k_2=q$ and the interaction vertices have the form

$$W^{\mathrm{intra}}_1(k_1,k_2,q)=-i\lambda\sqrt{\frac{1}{2\delta\omega_1(q)N}}[\sin k_1-\sin k_2]g^{-}_{12}, \tag{B20}$$

$$W^{\mathrm{intra}}_2(k_1,k_2,q)=-\lambda\sqrt{\frac{1}{2\delta\omega_2(q)N}}[\sin k_1+\sin k_2]f^{+}_{12}, \tag{B21}$$

$$W^{\mathrm{inter}}_1(k_1,k_2,q)=i\lambda\sqrt{\frac{1}{2\delta\omega_1(q)N}}[\sin k_1-\sin k_2]f^{+}_{12}, \tag{B22}$$

$$W^{\mathrm{inter}}_2(k_1,k_2,q)=-\lambda\sqrt{\frac{1}{2\delta\omega_2(q)N}}[\sin k_1+\sin k_2]g^{-}_{12}. \tag{B23}$$

The two auxiliary functions $f^{+}_{12}$ and $g^{-}_{12}$ are defined in Eqs. (B15) and (B16), respectively, while the dispersions for acoustic and optic phonons are given in Appendix A, Eqs. (A17) and (A18).

Finally, the coupling to external light fields, Eq. (2), is recast into the form

$$\delta H_{\pi\ \mathrm{light}}=\sum_{k,\sigma}\overline{\mu^{(1)}}[p^{\dagger}_{k\sigma}p_{k\sigma}+h_{-k\sigma}h^{\dagger}_{-k\sigma}]\mathscr{E}(t) + \sum_{k,\sigma}[\overline{\mu^{(2)}}p^{\dagger}_{k\sigma}h^{\dagger}_{-k\sigma}+\mathrm{H.c.}]\mathscr{E}(t), \tag{B24}$$

with intra- and interband dipole moments defined, respectively, by

$$\overline{\mu^{(1)}}=\frac{e}{2t_0}, \tag{B25}$$

$$\overline{\mu^{(2)}}=-i\frac{e}{2t_0}. \tag{B26}$$

Due to scaling, the coupling constants (dipole moments) are given by the electron charge in units of $2t_0$. In the main part of this work we consider only interband processes, i.e., creation (annihilation) of particle-hole pairs due to interaction with light.

Finally, the total particle-hole Hamiltonian upon which we base our treatment of nonlinear optics of conjugated polymers reads

$$H=H_{\mathrm{MF}}+H^{0}_{\mathrm{ph}}+\delta H^{\mathrm{TDA}}_{e\text{-}e}+\delta H^{pp}_{e\text{-}e}+\delta H^{hh}_{e\text{-}e}+\delta H^{\mathrm{intra}}_{e\text{-ph}} + \delta H_{\pi\ \mathrm{light}}. \tag{B27}$$

If we disregard acoustic phonons in $H^{0}_{\mathrm{ph}}$ and $\delta H^{\mathrm{intra}}_{e\text{-ph}}$, intraband processes in $\delta H_{\pi\ \mathrm{light}}$, the zero-point motion of phonons, and the constant $E_{\mathrm{MFA}}$, this is identical to the Hamiltonian given by Eq. (4) in Sec. I.

## APPENDIX C: INTERACTION VERTICES OF THE COUPLED EPG

We give a brief account of the derivation of the interaction vertices defining the coupled EPG.[30] The Usui operator that formally maps fermionic operators onto bosonic operators is unitary. To obtain the bosonic version of the total Hamiltonian Eq. (16), we simply have to replace $S^\dagger_{K\nu}$, $C^\dagger_{kq}$, and $D^\dagger_{kq}$ by their respective boson expansions $(S^\dagger_{K\nu})_B$, $(C^\dagger_{kq})_B$, and $(D^\dagger_{kq})_B$. Therefore, employing Eqs. (23), (25), and (26), we find for the free particle-hole pair plus particle-hole scattering terms of Eq. (16)

$$\begin{aligned}
&\sum_k E_k[C^\dagger_{kk}+D^\dagger_{kk}]+\sum_{K,Q}\sum_{\nu,\mu} V^{\mathrm{TDA}}_{\nu\mu}(K)\,\delta_{KQ}S^\dagger_{K\nu}S_{Q\mu}\\
&\quad\to\sum_{K,\nu,\mu}\sum_{r,q}\Phi^\nu_K(q)[(E_{K/2+q}+E_{K/2-q})\,\delta_{qr}\\
&\qquad+G_K(qr)]\Phi^\mu_K(r)A^\dagger_{K\nu}A_{K\mu}\\
&\qquad-\frac{1}{4}\sum_{K_i,\nu_i}\delta_{K_1+K_2,K_3+K_4}\sum_\nu V^{TDA}_{\nu_1\nu}(K_1)\\
&\qquad\times Y(K_1\nu;K_4\nu_4K_3\nu_3K_2\nu_2)A^\dagger_{K_1\nu_1}A^\dagger_{K_2\nu_2}A_{K_3\nu_3}A_{K_4\nu_4}\\
&\qquad-\frac{1}{4}\sum_{K_i,\nu_i}\delta_{K_1+K_2,K_3+K_4}\sum_\nu V^{\mathrm{TDA}}_{\nu_4\nu}(K_4)\\
&\qquad\times Y(K_4\nu;K_1\nu_1K_2\nu_2K_3\nu_3)\\
&\qquad\times A^\dagger_{K_1\nu_1}A^\dagger_{K_2\nu_2}A_{K_3\nu_3}A_{K_4\nu_4}. \qquad \text{(C1)}
\end{aligned}$$

By choosing the exciton wave function $\Phi^\nu_K$ to be *real*, we already anticipated that we take $\Phi^\nu_K$ as the solution of the *symmetric* eigenvalue problem

$$\begin{aligned}
&\sum_r[(E_{K/2+q}+E_{K/2-q})\,\delta_{qr}+G_K(qr)]\Phi^\mu_K(r)\\
&\quad=\Omega_\mu(K)\Phi^\mu_K(q), \qquad \text{(C2)}
\end{aligned}$$

with the symmetric $(N/2\times N/2)$ matrix $G_K(rq)$ defined in Eq. (19). It can be shown that Eq. (C2) is equivalent to the solution of the two-time Green function for singlet particle-hole pairs in the TDA.[30] With the help of Eq. (C2) we can then rewrite $V^{\mathrm{TDA}}$, Eq. (18), in a very compact form

$$V^{\mathrm{TDA}}_{\nu\mu}(K)=\sum_q[\Omega_\mu(K)-E_{K/2+q}-E_{K/2-q}]\Phi^\nu_K(q)\Phi^\mu_K(q) \qquad \text{(C3)}$$

and the first term on the rhs of Eq. (C1) becomes diagonal. More specifically, we obtain, employing the orthogonality of the exciton wave functions $\Phi^\nu_K$,

$$\begin{aligned}
&\sum_{K,\nu,\mu}\sum_{r,q}\Phi^\nu_K(q)[(E_{K/2+q}+E_{K/2-q})\,\delta_{qr}\\
&\qquad+G_K(qr)]\Phi^\mu_K(r)A^\dagger_{K\nu}A_{K\mu}\\
&\qquad\to\sum_{K,\nu}\Omega_\nu(K)A^\dagger_{K\nu}A_{K\nu}. \qquad \text{(C4)}
\end{aligned}$$

Consequently, the first term on the rhs of Eq. (C1) describes bare TDA excitons, i.e., it is the leading term at vanishing pair density. The next two terms on the rhs of Eq. (C1) couple TDA excitons and originate from the Pauli exclusion principle. In this sense, these terms constitute purely *kinematic* effects.[31]

Again using Eqs. (25) and (26), we find, after normal ordering of the boson operators, for the interaction between particles in the conduction band [fourth and fifth terms of Eq. (16)]

$$\begin{aligned}
&\frac{1}{2N}\sum_{k_i}V^{pp}_{1234}C^\dagger_{k_1k_4}C^\dagger_{k_2k_3}-\frac{1}{2N}\sum_{k_i}V^{pp}_{1234}\delta_{k_2k_4}C^\dagger_{k_1k_3}\\
&\quad\to\frac{1}{2N}\sum_{K_i,\nu_i}\delta_{K_1+K_2,K_3+K_4}\\
&\qquad\times\sum_{kq}V^{pp}(K_1-K_3+k,K_2-K_4+q,q,k)\\
&\qquad\times P^-_{K_1\nu_1;K_3\nu_3}(K_1-K_3+k,k)P^-_{K_2\nu_2;K_4\nu_4}\\
&\qquad\times(K_2-K_4+q,q)A^\dagger_{K_1\nu_1}A^\dagger_{K_2\nu_2}A_{K_3\nu_3}A_{K_4\nu_4} \qquad \text{(C5)}
\end{aligned}$$

and, similarly for the interaction among holes in the valence band [sixth and seventh terms of Eq. (16)],

$$\begin{aligned}
&\frac{1}{2N}\sum_{k_i}V^{hh}_{1234}D^\dagger_{-k_3-k_2}D^\dagger_{-k_4-k_1}-\frac{1}{2N}\sum_{k_i}V^{hh}_{1234}\delta_{k_2k_4}D^\dagger_{-k_3-k_1}\\
&\quad\to\frac{1}{2N}\sum_{K_i\nu_i}\delta_{K_1+K_2,K_3+K_4}\sum_{k,q}V^{hh}(k,q,K_3-K_1+q,K_4\\
&\qquad-K_2+k)P^+_{K_1\nu_1;K_3\nu_3}(K_1-K_3-q,-q)\\
&\qquad\times P^+_{K_2\nu_2;K_4\nu_4}(K_2-K_4-k,-k)\\
&\qquad\times A^\dagger_{K_1\nu_1}A^\dagger_{K_2\nu_2}A_{K_3\nu_3}A_{K_4\nu_4}. \qquad \text{(C6)}
\end{aligned}$$

In contrast to the two-body terms of Eq. (C1), these coupling terms originate from both the Pauli principle and the underlying Coulomb interaction. In this sense, Eqs. (C5) and (C6) contain *kinematic* as well as *dynamic* processes. Collecting terms, we finally obtain, for the exciton-exciton interaction (numerical indices stand for $K\nu$),

$$\mathscr{H}_{\rm int}^{\rm ex\text{-}ex}=\sum_{K_i,\nu_i}\delta_{K_1+K_2,K_3+K_4}\mathscr{W}_{1234}A_1^\dagger A_2^\dagger A_3 A_4, \quad \text{(C7)}$$

with the exciton-exciton vertex defined by

$$\begin{aligned}W_{1234}&\equiv W(K_1\nu_1K_2\nu_2K_3\nu_3K_4\nu_4)\\&=-\frac{1}{4}\sum_\nu V^{\rm TDA}_{\nu_1\nu}(K_1)Y(K_1\nu;K_4\nu_4K_3\nu_3K_2\nu_2)\\&\quad-\frac{1}{4}\sum_\nu V^{\rm TDA}_{\nu_4\nu}(K_4)Y(K_4\nu;K_1\nu_1K_2\nu_2K_3\nu_3)\\&\quad+\frac{1}{2N}\sum_{k,q}V^{pp}(K_1-K_3+k,K_2-K_4+q,q,k)\\&\quad\times P^-_{K_1\nu_1;K_3\nu_3}(K_1-K_3+k,k)P^-_{K_2\nu_2;K_4\nu_4}\\&\quad\times(K_2-K_4+q,q)+\frac{1}{2N}\sum_{k,q}V^{hh}(k,q,K_3-K_1\\&\quad+q,K_4-K_2+k)P^+_{K_1\nu_1;K_3\nu_3}(K_1-K_3-q,-q)\\&\quad\times P^+_{K_2\nu_2;K_4\nu_4}(K_2-K_4-k,-k). \quad \text{(C8)}\end{aligned}$$

The interaction vertices $V^{(\,)}(\,)$ are defined in Appendix B, Eqs. (B7)–(B11), whereas $V^{\rm TDA}$ is given in Eq. (C3). The rearrangement coefficient $Y$ and the structure coefficients $P^\pm$ are denoted in Eqs. (24), (14), and (15), respectively. To clarify the physical content, we visualize Eq. (C8) in Fig. 3 employing mode-mode coupling diagrams.[32]

Next, with the help of Eqs. (25) and (26), it is easy to express the coupling between particles (holes) and optical phonons in terms of boson operators. Considering only intraband processes we write

$$\begin{aligned}&\sum_{k_1,k_2,q}W_2^{\rm intra}(k_1,k_2,q)(b_q+b^\dagger_{-q})[C^\dagger_{k_1k_2}+D^\dagger_{-k_2,-k_1}]\\&\quad\to\sum_{K,Q}\sum_{\nu,\mu}\mathscr{M}_{\nu\mu}(K;Q)A^\dagger_{K+Q\nu}A_{K\mu}(B_Q+B^\dagger_{-Q}), \quad \text{(C9)}\end{aligned}$$

with the exciton-phonon vertex given by

$$\begin{aligned}\mathscr{M}_{\nu\mu}(K;Q)&=\sum_k W_2^{\rm intra}(k+Q,k,Q)P^-_{K+Q\nu;K\mu}(k+Q,k)\\&\quad+\sum_k W_2^{\rm intra}(k+Q,k,Q)\\&\quad\times P^+_{K+Q\nu;K\mu}(-k,-k-Q) \quad \text{(C10)}\end{aligned}$$

and $W_2^{\rm intra}(k_1,k_2,q)$ defined in Eq. (B21). The first term in Eq. (C9) originates form scattering processes between phonons and particles in the conduction band, whereas the second term arises from scattering of phonons on holes in the valence band. Furthermore, translational invariance restricts phonon and exciton momenta. The internal quantum number $\nu$ of an exciton is, however, unconstrained. Considering $\nu$ as a ''band index,'' this means that we have both scattering events within a band ($\nu=\mu$, intraband) and between bands ($\nu\neq\mu$, interband). With the exciton-phonon vertex defined in Eq. (C10), we write, for the exciton-phonon coupling,

$$\mathscr{H}_{\rm int}^{\rm ex\text{-}ph}=\sum_{K,Q}\sum_{\nu,\mu}\mathscr{M}_{\nu\mu}(K;Q)A^\dagger_{K+Q\nu}A_{K\mu}(B_Q+B^\dagger_{-Q}). \quad \text{(C11)}$$

Figure 4 represents the exciton-phonon vertex in terms of mode-mode coupling diagrams.

Finally, using the expansion (23), we obtain for the matter-light coupling, taking into account only interband transitions resulting in either the creation or annihilation of excitons,

$$\begin{aligned}-\sum_\nu(\mu_\nu S_{0\nu}+\text{H.c.})\mathscr{E}(t)&\to-\sum_\nu(\mu_\nu A_{0\nu}+\text{H.c.})\mathscr{E}(t)\\&\quad+\sum_{K_i,\nu_i}\tilde{\mu}(K_1\nu_1K_2\nu_2K_3\nu_3)\\&\quad\times\delta_{K_3,K_1+K_2}[A^\dagger_{K_1\nu_1}A^\dagger_{K_2\nu_2}\\&\quad\times A_{K_3\nu_3}+\text{H.c.}]\mathscr{E}(t), \quad \text{(C12)}\end{aligned}$$

with the nonlinear exciton-light vertex written as

$$\tilde{\mu}(K_1\nu_1K_2\nu_2K_3\nu_3)=\frac{1}{4}\sum_\nu\mu_\nu Y(0\nu;K_1\nu_1K_2\nu_2K_3\nu_3) \quad \text{(C13)}$$

and the rearrangement coefficient $Y$ given by Eq. (24). The first term on the rhs of (C12) does not modify the material system and gives rise to linear absorption in the TDA (viz., the Elliott formula for absorption[33]). In contrast, the second (nonlinear) coupling term leads to self-energy corrections, thus modifying the material system. In terms of bosons, it is this term that describes the so-called phase-space-filling effect.[33] Thus exciton-light coupling consists of two terms explicitly given by

$$\begin{aligned}\mathscr{H}_{\rm int}^{\rm ex\text{-}light}&=\mathscr{H}_{\rm int}^{\rm ex\text{-}light,L}+\mathscr{H}_{\rm int}^{\rm ex\text{-}light,NL}\\&=-\sum_\nu(\mu_\nu A_{0\nu}+\text{H.c.})\mathscr{E}(t)\\&\quad+\sum_{K_i,\nu_i}\tilde{\mu}(K_1\nu_1K_2\nu_2K_3\nu_3)\delta_{K_3,K_1+K_2}\\&\quad\times[A^\dagger_{K_1\nu_1}A^\dagger_{K_2\nu_2}A_{K_3\nu_3}+\text{H.c.}]\mathscr{E}(t). \quad \text{(C14)}\end{aligned}$$

In Fig. 5 we depict linear and nonlinear exciton-light coupling in terms of mode-mode coupling diagrams. Attaching the free optic phonon and exciton Hamiltonians to Eqs. (C7), (C11), and (C14), we obtain the EPG Hamiltonian

$$\begin{aligned}\mathscr{H}&=\sum_{K,\nu}\Omega_\nu(K)A^\dagger_{K\nu}A_{K\nu}+\sum_Q\omega(Q)B^\dagger_QB_Q\\&\quad+\mathscr{H}_{\rm int}^{\rm ex\text{-}ex}+\mathscr{H}_{\rm int}^{\rm ex\text{-}ph}+\mathscr{H}_{\rm int}^{\rm ex\text{-}light}. \quad \text{(C15)}\end{aligned}$$

Neglecting contributions from acoustic phonons, we finally find the EPG model as displayed in Sec. II, Eq. (27).

*Present address: Centre de Recherches sur les Très Basses Températures, Centre National de la Recherche Scientifique, Boîte Postale 166, 38042 Grenoble, Cédex 9, France.
[1] P.D. Townsend *et al.*, Appl. Phys. Lett. **53**, 1782 (1988).
[2] P.D. Townsend *et al.*, Appl. Phys. Lett. **55**, 1829 (1989).
[3] D.D.C. Bradley *et al.*, Synth. Met. **29**, E121 (1989); J.H. Burroughes *et al.*, Nature **347**, 539 (1990).
[4] G.J. Blanchard *et al.*, Phys. Rev. Lett. **63**, 887 (1989).
[5] T.W. Hagler *et al.*, Phys. Rev. B **44**, 8652 (1991).
[6] J.W.P. Hsu *et al.*, Phys. Rev. B **49**, 712 (1994).
[7] See, e.g., D.S. Chemla, J.-Y. Bigot, M.-A. Mycek, and S. Weiss, Phys. Rev. B **50**, 8439 (1994); D.-S. Kim *et al.*, Phys. Rev. Lett. **69**, 2725 (1992); S. Weiss *et al.*, *ibid.* **69**, 2685 (1992).
[8] B.I. Greene *et al.*, Phys. Rev. Lett. **61**, 325 (1988).
[9] G.J. Blanchard *et al.*, J. Chem. Phys. **93**, 4377 (1990).
[10] S. Schmitt-Rink, D.S. Chemla, and D.A.B. Miller, Adv. Phys. **38**, 89 (1989).
[11] B.J. Orr and J.F. Ward, Mol. Phys. **20**, 513 (1971).
[12] H. Sakamoto and T. Kishimoto, Nucl. Phys. A **486**, 1 (1988).
[13] The description of excitons in terms of boson operators started with the work of E. Hanamura. In these seminal papers, he employed a boson mapping that in many respects is a precursor to Ref. 12. E. Hanamura, J. Phys. Soc. Jpn. **29**, 50 (1970); Solid State Commun. **11**, 485 (1972); J. Phys. Soc. Jpn. **37**, 1545 (1974); **29**, 50 (1974).
[14] S. Schmitt-Rink and D.S. Chemla, Phys. Rev. Lett. **57**, 2752 (1986); S. Schmitt-Rink, D.S. Chemla, and H. Haug, Phys. Rev. B **37**, 941 (1988).
[15] A. Griffin, *Excitations in Bose-Condensed Liquids* (Cambridge University Press, Cambridge, England, 1993).
[16] H. Hayashi and K. Nasu, Phys. Rev. B **32**, 5295 (1985).
[17] See, e.g., *Handbook of Conducting Polymers Vol. I*, edited by T.A. Skotheim (Dekker, New York, 1986).
[18] V.A. Shakin and S. Abe, Phys. Rev. B **50**, 4306 (1994).
[19] W.-P. Su, R.J. Schrieffer, and A. J. Heeger, Phys. Rev. Lett. **42**, 1698 (1979); M.J. Rice, Phys. Lett. **71A**, 152 (1979).
[20] Z.G. Soos *et al.*, Phys. Rev. B **47**, 1742 (1993).
[21] Y. Toyozawa, Prog. Theor. Phys. **12**, 421 (1954).
[22] E. Hanamura and H. Haug, Phys. Rep. **33**, 209 (1977).
[23] A.L. Fetter and J.D. Walecka, *Quantum Theory of Many Particle Systems* (McGraw-Hill, New York, 1971).
[24] H. Haug, Phys. Status Solidi B **173**, 139 (1992); L. Bányai *et al.*, *ibid.* **173**, 149 (1992).
[25] M. Nakahara and K. Maki, Synth. Met. **13**, 149 (1986).
[26] I. Batistić and A. R. Bishop, Phys. Rev. B **45**, 5282 (1992).
[27] H. Haug and S. Schmitt-Rink, Prog. Quantum Electron. **9**, 3 (1984).
[28] M. Lindberg and S.W. Koch, Phys. Rev. B **38**, 3342 (1988).
[29] T. Kishimoto and T. Tamura, Phys. Rev. C **27**, 341 (1983).
[30] F.X. Bronold, Ph.D. thesis, Universität Bayreuth, 1995.
[31] P. Ring and P. Schuck, *The Nuclear Many-Body Problem* (Springer-Verlag, Berlin, 1980).
[32] P. Ring and P. Schuck, Phys. Rev. C **16**, 801 (1977).
[33] H. Haug and S.W. Koch, *Quantum Theory of the Optical and Electronic Properties of Semiconductors* (World Scientific, Singapore, 1990).
[34] R. Zimmermann, Phys. Status Solidi B **146**, 545 (1988); R. Zimmermann and M. Hartmann, *ibid.* **150**, 365 (1988).
[35] J.-P. Blaizot and G. Ripka, *Quantum Theory of Finite Systems* (MIT Press, Cambridge, MA, 1986).
[36] N. Bogoliubov, J. Phys. (Moscow) **11**, 23 (1947).
[37] D.-S. Kim *et al.*, Phys. Rev. Lett. **68**, 1006 (1992).
[38] N. Ullah and D.J. Rowe, Nucl. Phys. A **163**, 257 (1971).
[39] W.J. Jones and B.P. Stoicheff, Phys. Rev. Lett. **13**, 657 (1964); S. Saikan *et al.*, J. Chem. Phys. **82**, 5409 (1985).
[40] N. Bloembergen, *Nonlinear Optics* (Benjamin, New York, 1964).
[41] S. Mukamel *et al.*, Science **265**, 250 (1994); A. Takahashi and S. Mukamel, J. Chem. Phys. **100**, 2366 (1994); M. Hartmann, A. Takahashi, S. Mukamel, and M. Schreiber (unpublished).
[42] A.L. Ivanov and L.V. Keldysh, Zh. Eksp. Teor. Fiz. **84**, 404 (1982); A.L. Ivanov, *ibid.* **90**, 158 (1986).
[43] W.B. Bosma *et al.*, Phys. Rev. Lett. **68**, 2456 (1992).
[44] M. Kuwata-Gonokami *et al.*, Nature **367**, 47 (1994).
[45] V.G. Pedrocchi and T. Tamura, Phys. Rev. C **29**, 1461 (1984); M.B. Jamaluddin *et al.*, J. Phys. G **15**, 977 (1989).